29. Nikolenko, G. N., S. Palmer, F. Maldarelli, J. W. Mellors, J. M. Coffin, and V. K. Pathak. Mechanism for nucleoside analog-mediated abrogation of HIV-1 replication: balance between RNase H activity and nucleotide excision. *Proc Nat Acad Sci USA.* 2005, **102**:2093-2098.

30. Ohrui, H., S. Kohgo, H. Hayakawa, E. Kodama, M. Matsuoka, T. Nakata, and H. Mitsuya. 2'-Deoxy-4'-C-ethynyl-2-fluoroadenosine: a nucleoside reverse transcriptase inhibitor with highly potent activity against all HIV-1 strains, favorable toxic profiles and stability in plasma. *Nucleic Acids Symp Ser (Oxf)* 2006, 1-2.

31. Ren, J., R. Esnouf, A. Hopkins, C. Ross, Y. Jones, D. Stammers, and D. Stuart. The structure of HIV-1 reverse transcriptase complexed with 9-chloro-TIBO: lessons for inhibitor design. *Structure.* 1995, **3**:915-926.

32. Ren, J., C. Nichols, L. Bird, P. Chamberlain, K. Weaver, S. Short, D. I. Stuart, and D. K. Stammers. Structural mechanisms of drug resistance for mutations at codons 181 and 188 in HIV-1 reverse transcriptase and the improved resilience of second generation non-nucleoside inhibitors. *J Mol Biol.* 2001, **312**:795-805.

33. Sarafianos, S. G., A. D. Clark, Jr., S. Tuske, C. J. Squire, K. Das, D. Sheng, P. Ilankumaran, A. R. Ramesha, H. Kroth, J. M. Sayer, D. M. Jerina, P. L. Boyer, S. H. Hughes, and E. Arnold. Trapping HIV-1 reverse transcriptase before and after translocation on DNA. *J Biol Chem.* 2003, **278:**16280-16288.

34. Sarafianos, S. G., K. Das, A. D. Clark, Jr., J. Ding, P. L. Boyer, S. H. Hughes, and E. Arnold. Lamivudine (3TC) resistance in HIV-1 reverse transcriptase involves steric hindrance with beta-branched amino acids. *Proc Nat Acad Sci USA.* 1999, **96**:10027-10032.

35. Sarafianos, S. G., K. Das, S. H. Hughes, and E. Arnold. Taking aim at a moving target: designing drugs to inhibit drug-resistant HIV-1 reverse transcriptases. *Curr Opin Struct Biol.* 2004, **14**:716-730.

36. Sarafianos, S. G., S. H. Hughes, and E. Arnold. Designing anti-AIDS drugs targeting the major mechanism of HIV-1 RT resistance to nucleoside analog drugs. *Int J Biochem Cell Biol.* 2004, **36**:1706-1715.

37. Sarafianos, S. G., B. Marchand, K. Das, D. M. Himmel, M. A. Parniak, S. H. Hughes, and E. Arnold. Structure and function of HIV-1 reverse transcriptase: molecular mechanisms of polymerization and inhibition. *J Mol Biol.* 2009, **385**:693-713.

38. Schuckmann, M. M., B. Marchand, A. Hachiya, E. N. Kodama, K. A. Kirby, K. Singh, and S. G. Sarafianos. The N348I mutation at the connection subdomain of HIV-1 reverse transcriptase decreases binding to nevirapine. *J Biol Chem* **285**:38700-38709.

39. Singh, K., B. Marchand, K. A. Kirby, E. Michailidis, and S. G. Sarafianos. 2010. Structural Aspects of Drug Resistance and Inhibition of HIV-1 Reverse Transcriptase. Viruses **2**:606-638.

40. Sluis-Cremer, N., D. Arion, and M. A. Parniak. 2000. Molecular mechanisms of HIV-1 resistance to nucleoside reverse transcriptase inhibitors (NRTIs). *Cell Mol Life Sci.* **57**:1408-1422.

41. Smerdon, S. J., J. Jager, J. Wang, L. A. Kohlstaedt, A. J. Chirino, J. M. Friedman, P. A. Rice, and T. A. Steitz. 1994. Structure of the binding site for nonnucleoside inhibitors of the reverse transcriptase of human immunodeficiency virus type 1. *Proc Nat Acad Sci USA.* **91**:3911-3915.

42. Wang, J., S. J. Smerdon, J. Jager, L. A. Kohlstaedt, P. A. Rice, J. M. Friedman, and T. A. Steitz. 1994. Structural basis of asymmetry in the human immunodeficiency virus type 1 reverse transcriptase heterodimer. *Proc Nat Acad Sci USA.* **91**:7242-7246.

43. Yap, S. H., C. W. Sheen, J. Fahey, M. Zanin, D. Tyssen, V. D. Lima, B. Wynhoven, M. Kuiper, N. Sluis-Cremer, P. R. Harrigan, and G. Tachedjian. 2007. N348I in the connection domain of HIV-1 reverse transcriptase confers zidovudine and nevirapine resistance. *PLoS Med* **4**:e335.

44. Singh, M. P., and Kumar, V., Biodegradation of vegetable and agrowastes by *Pleurotus sapidus*: A noble strategy to produce mushroom with enhanced yield and nutrition. *Cell. Mol. Biol.* 2012, **58** (1): 1-7.

45. Pandey, V. K., Singh, M.P., Srivastava, A. K., Vishwakarma S. K., and Takshak, S., Biodegradation of sugarcane bagasse by white rot fungus *Pleurotus citrinopileatus. Cell. Mol. Biol.* 2012, **58** (1): 8-14.

46. Ruhal, A., Rana, J. S., Kumar S., and Kumar, A., Immobilization of malate dehydrogenase on carbon nanotubes for development of malate biosensor. *Cell. Mol. Biol.* 2012, **58** (1): 15-20.

47. Vishwakarma, S. K., Singh, M. P., Srivastava A.K. and Pandey, V. K., Azo dye (direct blue) decolorization by immobilized extracellular enzymes of *Pleurotus* species. *Cell. Mol. Biol.* 2012, **58** (1): 21-25.

48. Dash, S. K., Sharma, M., Khare, S. and Kumar, A., *rmpM* gene as a genetic marker for human bacterial meningitis. *Cell. Mol. Biol.* 2012, **58** (1): 26-30.

49. Bertoletti, F., Crespan, E. and Maga, G., Tyrosine kinases as essential cellular cofactors and potential therapeutic targets for human immunodeficiency virus infection. *Cell. Mol. Biol.* 2012, **58** (1): 31-43.

50. Sandalli, C., Singh, K., and Modak, M. J., Characterization of catalytic carboxylate triad in non-replicative DNA polymerase III (pol E) of *Geobacillus kaustophilus* HTA. *Cell. Mol. Biol.* 2012, **58** (1): 44-49.

51. Kaushal, A., Kumar, D., Khare, S. and Kumar, A., *speB* gene as a specific genetic marker for early detection of rheumatic heart disease in human. *Cell. Mol. Biol.* 2012, **58** (1): 50-54.

52. Datta, J. and Lal, N., Application of molecular markers for genetic discrimination of *fusarium* wilt pathogen races affecting chickpea and pigeonpea in major regions of India. *Cell. Mol. Biol.* 2012, **58** (1): 55-65.

53. Siddiqi, N. J., Alhomida, A. S., Khan, A. H. and Onga, W.Y., Study on the distribution of different carnitine fractions in various tissues of bovine eye. *Cell. Mol. Biol.* 2012, **58** (1): 66-70.

54. Ong, Y. T., Kirby, K. A., Hachiya, A., Chiang, L. A., Marchand, B., Yoshimura, K., Murakami, T., Singh, K., Matsushita, S. and Sarafianos, S. G., Preparation of biologically active single-chain variable antibody fragments that target the HIV-1 GP120 v3 loop. *Cell. Mol. Biol.* 2012, **58** (1): 71-79.

55. Singh, J., Gautam, S. and Bhushan Pant, A., Effect of UV-B radiation on UV absorbing compounds and pigments of moss and lichen of Schirmacher Oasis region, East Antarctica. *Cell. Mol. Biol.* 2012, **58** (1): 80-84.

56. Singh, V. P., Srivastava, P. K., and Prasad, S. M., Impact of low and high UV-B radiation on the rates of growth and nitrogen metabolism in two cyanobacterial strains under copper toxicity. *Cell. Mol. Biol.* 2012, **58** (1): 85-95.

57. Datta, J. and Lal, N., Temporal and spatial changes in phenolic compounds in response *Fusarium* wilt in chickpea and pigeonpea. *Cell. Mol. Biol.* 2012, **58** (1): 96-102.

58. Sharma, R. K., JAISWAL, S. K., Siddiqi, N. J., and Sharma, B., Effect of carbofuran on some biochemical indices of human erythrocytes *in vitro. Cell. Mol. Biol.* 2012, **58** (1): 103-109.

59. Singh, A. K., Singh, S. and Singh, M. P., Bioethics A new frontier of biological Science. *Cell. Mol. Biol.* 2012, **58** (1): 110-114.

60. Adedeji, A. O., Singh, K. and Sarafianos, S. G., Structural and biochemical basis for the difference in the helicase activity of two different constructs of SARS-CoV helicase. *Cell. Mol. Biol.* 2012, **58** (1): 115-121.

61. Singh, S., Choudhuri, G., Kumar, R. and Agarwal, S., Association of 5, 10-methylenetetrahydrofolate reductase C677T polymorphism in susceptibility to tropical chronic pancreatitis in North Indian population. *Cell. Mol. Biol.* 2012, **58** (1): 122-127.

62. Sharma, R. K., Rai, K. D. and Sharma, B., *In* vitro carbofuran induced micronucleus formation in human blood lymphocytes. *Cell. Mol. Biol.* 2012, **58** (1): 128-133.

63. Naraian, R., Ram, S., Kaistha S. D. and Srivastava J., Occurrence of plasmid linked multiple drug resistance in bacterial isolates of tannery effluent. *Cell. Mol. Biol.* 2012, **58** (1): 134-141.

64. Pandey, A. K., Mishra, A. K., And Mishra, A., Antifungal and an-

tioxidative potential of oil and extracts, respectively derived from leaves of Indian spice plant *Cinnamomum tamala. Cell. Mol. Biol.* 2012, **58** (1): 142-147.

65. Mishra, N., and Rizvi, S. I., Quercetin modulates na/k atpase and sodium hydrogen exchanger in type 2 diabetic erythrocytes. *Cell. Mol. Biol.* 2012, **58** (1): 148-152.

66. Kumar, A., Sharma, B. and Pandey, R. S., Assessment of stress in effect to pyrethroid insecticides, λ-cyhalothrin and cypermethrin in a freshwater fish, *Channa punctatus* (Bloch). *Cell. Mol. Biol.* 2012, **58** (1): 153-159.

67. Srivastava N., Sharma, R. K., Singh, N. and Sharma, B., Acetylcholinesterase from human erythrocytes membrane: a screen for evaluating the activity of some traditional plant extracts. *Cell. Mol. Biol.* 2012, **58** (1): 160-169.

68. Singh, M.P., Pandey, A. K., Vishwakarma S. K., Srivastava, A. K. and Pandey, V. K., Extracellular Xylanase Production by *Pleurotus* species on Lignocellulosic Wastes under *in vivo* Condition using Novel Pretreatment. *Cell. Mol. Biol.* 2012, **58** (1): 170-173.

69. Kumar, S., Sharma, U. K., Sharma, A. K., Pandey, A. K., Protective efficacy of *Solanum xanthocarpum* root extracts against free radical damage: phytochemical analysis and antioxidant effect. *Cell. Mol. Biol.* 2012, **58** (1): 174-181.

70. Shukla, A., Singh, A., Singh, A., Pathak, L.P., Shrivastava, N., Tripathi, P. K., Singh, K. and Singh, M.P., Inhibition of *P. falciparum* pfATP6 by curcumin and its derivatives: A bioinformatic Study. *Cell. Mol. Biol.* 2012, **58** (1): 182-186.

71. Parveen, A., Rizvi, S. H. M., Gupta, A., Singh, R., Ahmad, I., Mahdi, F., and Mahdi, A. A., NMR-based metabonomics study of sub-acute hepatotoxicity induced by silica nanoparticles in rats after intranasal exposure. *Cell. Mol. Biol.* 2012, **58** (1): 196-203.

The International Journal of Biochemistry & Cell Biology 45 (2013) 908–915

Contents lists available at SciVerse ScienceDirect

The International Journal of Biochemistry & Cell Biology

journal homepage: www.elsevier.com/locate/biocel

Mechanism of resistance to S138A substituted enfuvirtide and its application to peptide design

Kazuki Izumi[a], Kumi Kawaji[b], Fusasko Miyamoto[b], Kazuki Shimane[a], Kazuya Shimura[a], Yasuko Sakagami[a], Toshio Hattori[b], Kentaro Watanabe[c], Shinya Oishi[c], Nobutaka Fujii[c], Masao Matsuoka[a], Mitsuo Kaku[d], Stefan G. Sarafianos[e,f], Eiichi N. Kodama[a,b,d,*]

[a] *Laboratory of Virus Control, Institute for Virus Research, Kyoto University, 53 Shogoin Kawaramachi, Sakyo-ku, Kyoto 606-8507, Japan*
[b] *Division of Emerging Infectious Diseases, Tohoku University School of Medicine, Sendai 980-8575, Japan*
[c] *Department of Bioorganic Medical Chemistry, Division of Physical and Organic Chemistry, Graduate School of Pharmaceutical Sciences, Kyoto University, 46-29 Yoshida Shimoadachi-cho, Sakyo-ku, Kyoto 606-8501, Japan*
[d] *Division of Infection Control and Laboratory Diagnostics, Tohoku University School of Medicine, Sendai 980-8575, Japan*
[e] *Christopher S. Bond Life Sciences Center, Department of Molecular Microbiology and Immunology, University of Missouri School of Medicine, Columbia, MO, USA*
[f] *Department of Biochemistry, University of Missouri School of Medicine, Columbia, MO, USA*

ARTICLE INFO

Article history:
Received 31 October 2012
Received in revised form 15 January 2013
Accepted 20 January 2013
Available online 26 January 2013

Keywords:
Resistance
HIV-1
gp41
T-20
Mutation
Fusion inhibitor

ABSTRACT

T-20 (enfuvirtide) resistance is caused by the N43D primary resistance mutation at its presumed binding site at the N-terminal heptad repeat (N-HR) of gp41, accompanied by the S138A secondary mutation at the C-terminal HR of gp41 (C-HR). We have discovered that modifying T-20 to include S138A (T-20_{S138A}) allows it to efficiently block wild-type and T20-resistant viruses, by a mechanism that involves improved binding of T-20_{S138A} to the N-HR that contains the N43D primary mutation. To determine how HIV-1 in turn escapes T-20_{S138A} we used a dose escalation method to select T-20_{S138A}-resistant HIV-1 starting with either wild-type (HIV-1_{WT}) or T-20-resistant (HIV-$1_{N43D/S138A}$) virus. We found that when starting with WT background, I37N and L44M emerged in the N-HR of gp41, and N126K in the C-HR. However, when starting with HIV-$1_{N43D/S138A}$, L33S and I69L emerged in N-HR, and E137K in C-HR. T-20_{S138A}-resistant recombinant HIV-1 showed cross-resistance to other T-20 derivatives, but not to C34 derivatives, suggesting that T-20_{S138A} suppressed HIV-1 replication by a similar mechanism to T-20. Furthermore, E137K enhanced viral replication kinetics and restored binding affinity with N-HR containing N43D, indicating that it acts as a secondary, compensatory mutation. We therefore introduced E137K into T-20_{S138A} (T-$20_{E137K/S138A}$) and revealed that T-$20_{E137K/S138A}$ moderately suppressed replication of T-20_{S138A}-resistant HIV-1. T-$20_{E137K/S138A}$ retained activity to HIV-1 without L33S, which seems to be a key mutation for T-20 derivatives.

Our data demonstrate that secondary mutations can be consistently used for the design of peptide inhibitors that block replication of HIV resistant to fusion inhibitors.

1. Introduction

Human immunodeficiency virus type 1 (HIV-1) fusion to host cell membrane is mediated by formation of a six-helix bundle of the transmembrane subunit gp41 (Chan et al., 1997). Peptides corresponding to amino acid sequences of the gp41 carboxyl-terminal heptad repeat (C-HR) inhibit the HIV-1 fusion by acting as decoys and interfering with the formation of the six-helix bundle (Chan et al., 1998; Malashkevich et al., 1998). Although modified peptides such as SC34EK (Nishikawa et al., 2009), T-2635 (Dwyer et al., 2008), and D-peptides (Welch et al., 2007), and small molecules (Debnath et al., 1999) have been developed, T-20 (enfuvirtide) is the only fusion inhibitor approved for HIV therapy. It is a 36 amino acid peptide derived from the sequence of C-HR of gp41. It is thought to bind at the N-HR domain of gp41and interfere with the C-HR-N-HR interactions required for membrane fusion and injection of virus into the host cell. T-20 has potent anti-HIV-1 activity and effectively suppresses replication of HIV-1 *in vivo* (Kilby et al., 1998; Lalezari et al., 2003; Lazzarin et al., 2003). However, HIV-1 rapidly develops resistance through mutations in the amino-terminal HR (N-HR) of gp41, especially in the region between L33 and L45, which

* Corresponding author at: Division of Emerging Infectious Diseases, Tohoku University School of Medicine, Sendai 980-8575, Japan. Tel.: +81 22 717 7199; fax: +81 22 717 7199.
E-mail addresses: kodama515@med.tohoku.ac.jp, kodausa21@gmail.com (E.N. Kodama).

1357-2725/$ – see front matter © 2013 Elsevier Ltd. All rights reserved.
http://dx.doi.org/10.1016/j.biocel.2013.01.015

is thought to be the binding site of T-20 (Aquaro et al., 2006; Cardoso et al., 2007; He et al., 2008). Among these residues, N43D in the N-HR is one of the representative mutations for resistance to T-20 (Bai et al., 2008; Cabrera et al., 2006; Oliveira et al., 2009; Izumi et al., 2009; Ueno et al., 2009). Interestingly, most variants show impaired replication fitness, and thus often go on to acquire secondary mutations, such as S138A (Xu et al., 2005), in the C-HR region of gp41 that corresponds to the sequence of T-20. We and others have recently demonstrated that S138A functions as secondary resistance mutation and enhances resistance to T-20 by restoring impaired replication kinetics of T-20-resistant variants that contain primary mutations in the N-HR region, most notably N43D (Izumi et al., 2009; Watabe et al., 2009).

To preempt this escape strategy, we have previously designed a peptide analog of T-20 with the S138A change incorporated in it ($T\text{-}20_{S138A}$; Fig. 1A) and showed that this peptide significantly suppresses replication of T-20-resistant HIV-1 through enhancement of binding affinity to mutated N-HR, such as $N\text{-}HR_{N43D}$ (Izumi et al., 2009). Using circular dichroism (CD) and structural analyses, we also demonstrated that the S138A change provided increased stability to the six-helix bundle (Watabe et al., 2009). In subsequent studies, we validated our approach on another peptide-based fusion inhibitor, C34. In this case, we designed a variant of C34 carrying a secondary escape mutation, N126K, selected for the induction of C34 resistance (Nameki et al., 2005) and also present in HIV-1 isolates from T-20 experienced patients (Baldwin et al., 2004; Cabrera et al., 2006; Svicher et al., 2008). We showed that this C34 variant can effectively inhibit replication of C34-resistant HIV-1. These studies provided the proof of principle that it is possible to design improved peptide-based fusion inhibitors that are efficient against a major mechanism of drug resistance through introduction of resistance-associated mutation(s).

It remains unknown to this date how HIV-1 develops further resistance to $T\text{-}20_{S138A}$. Moreover, it is not known whether we can expand our strategy and modify $T\text{-}20_{S138A}$ to include the secondary mutation(s) that emerge during the selection of $T\text{-}20_{S138A}$-resistant HIV, resulting in a strategy that is applicable to the design of peptides customized to address viral resistance mutations. Hence, in the current study we selected $T\text{-}20_{S138A}$-resistant HIV-1 *in vitro* by a dose-escalating method. We revealed that the resistance mutations that emerged during selection experiments with wild-type or T-20-resistant HIV-1 are located in both the N-HR and the C-HR regions. Furthermore, the I37N and L33S mutations appeared to act as primary mutations for wild-type and T-20-resistant HIV-1, respectively. E137K, a C-HR mutation located in the T-20 sequence, improved replication kinetics and enhanced affinity to N-HR, indicating that E137K acts as a secondary mutation. Introducing the E137K change into the $T\text{-}20_{S138A}$ ($T\text{-}20_{E137K/S138A}$) resulted into a peptide inhibitor effective against $T\text{-}20_{S138A}$-resistant variants, suggesting that secondary or compensatory mutations can be widely applicable to the design of next generation peptide-based inhibitors that are active against HIV-1 resistant to earlier generation fusion-targeting drugs.

2. Materials and methods

2.1. Cells and viruses

MT-2 and 293T cells were grown in RPMI 1640 medium and Dulbecco's modified Eagle medium-based culture medium, respectively. HeLa-CD4-LTR-β-gal cells were kindly provided by Dr. M. Emerman through the AIDS Research and Reference Reagent Program, Division of AIDS, National Institute of Allergy and Infectious Disease (Bethesda, MD), and used for the drug susceptibility assay, as previously described (Nameki et al., 2005; Nishikawa et al., 2009). Recombinant infectious HIV-1 clones carrying various mutations were generated through site-directed mutagenesis of the pNL4-3 plasmid, as previously described (Nameki et al., 2005; Nishikawa et al., 2009). Each molecular clone was transfected into 293T cells with *Trans*IT (Madison, WI). After 48 h, the supernatants were harvested and stored at −80 °C.

2.2. Antiviral agents

The peptides used in this study (Fig. 1A) were chemically synthesized using standard Fmoc-based solid-phase techniques, as previously described (Oishi et al., 2008; Otaka et al., 2002). An HIV-1 reverse transcriptase inhibitor, 2′,3′-dideoxycytidine (ddC) was purchased from Sigma–Aldrich Japan (Tokyo, Japan) and used as a control.

2.3. Determination of drug susceptibility

Peptide sensitivity of infectious clones was determined by the multinuclear activation of galactosidase indicator (MAGI) assay as previously described (Nameki et al., 2005; Nishikawa et al., 2009). Briefly, the target cells (HeLa-CD4-LTR-β-gal; 10^4 cells/well) were plated in flat 96-well microtiter culture plates. On the following day, the cells were inoculated with the HIV-1 clones (60 MAGI units/well, resulting into 60 blue cells after 48 h incubation) and cultured in the presence of various concentrations of drugs in fresh medium. Forty-eight hours after virus exposure, all the blue cells stained with X-gal (5-bromo-4-chloro-3-indolyl-β-D-galactopyranoside) were counted in each well. The activity of test compounds was determined as the concentration that reduced HIV-1 infection by 50% (50% effective concentration [EC_{50}]).

2.4. Induction of HIV-1 variants resistant to $T\text{-}20_{S138A}$

MT-2 cells were exposed to HIV-1 and cultured in the presence of $T\text{-}20_{S138A}$. Cultures were incubated at 37 °C until an extensive cytopathic effect (CPE) was observed. The culture supernatants were used for further passages in MT-2 cells in the presence of two-fold increasing concentrations of $T\text{-}20_{S138A}$ when massive CPEs were seen in the earlier periods. Each passage usually took 5–7 days. The timing is highly dependent on the type of specific mutations introduced, as previously reported (Nameki et al., 2005; Shimura et al., 2010). For example, a passage that follows introduction of novel mutation(s) should shorten the passage period to perhaps 4–5 days. However, there will be longer delays for passages where there are no novel mutations or when there is appearance of only secondary mutations. The dose-escalation process was repeated until resistant variants were obtained. This selection was carried out for a total of 60 passages (approximately 1 year). At the indicated passages (Fig. 1B and C), the sequence of the *env* region was determined by direct sequencing of the proviral DNA extracted from the infected MT-2 cells.

2.5. Viral replication kinetics assay

MT-2 cells (10^5 cells/1 mL) were infected with each virus preparation (500 MAGI units) for 16 h. Infected cells were then washed and cultured in a final volume of 3 mL. The culture supernatants were collected on day 2 through day 5 post-infection, and amounts of p24 antigen were determined.

2.6. CD spectroscopy

Each peptide was incubated at 37 °C for 30 min (the final concentrations of peptides were 10 μM in phosphate buffered saline [PBS];

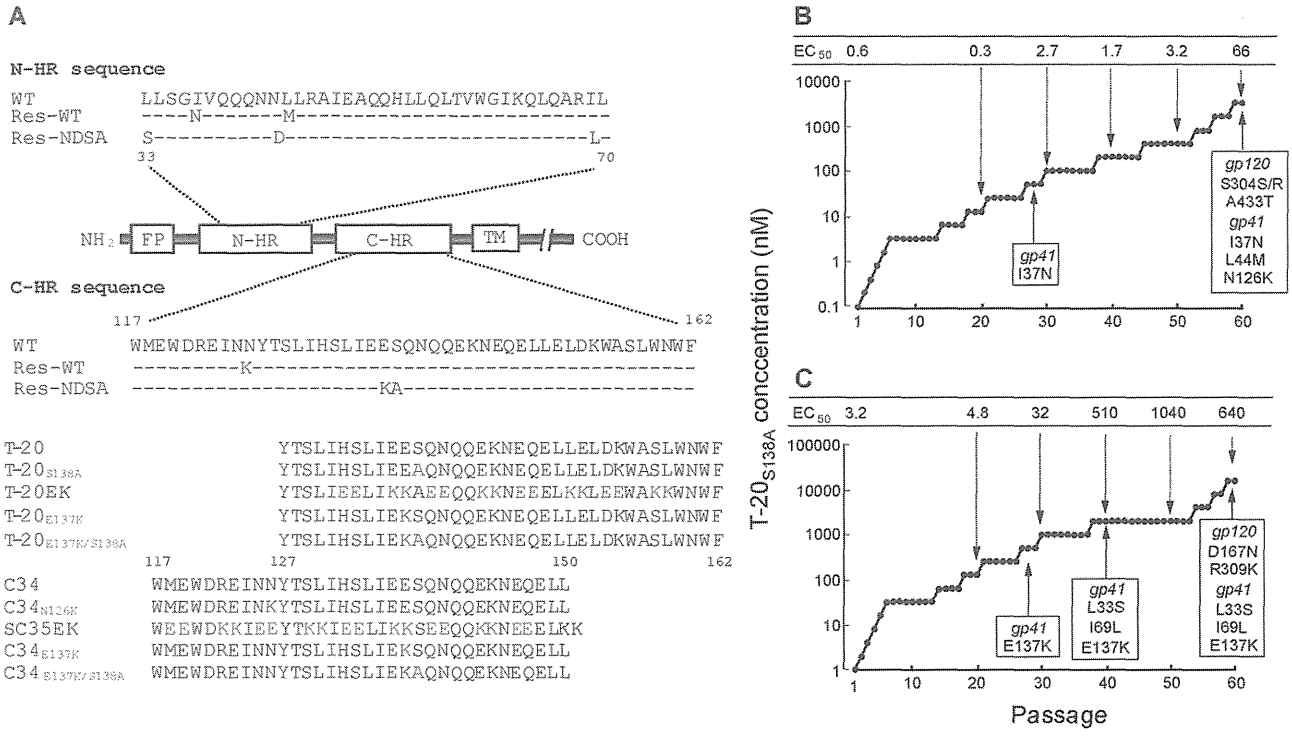

Fig. 1. Domains of gp41 and induction of T-20_{S138A}-resistant HIV-1. (A) Domains of gp41, substitutions observed during *in vitro* passage with T-20_{S138A}, and amino acid sequences of T-20- and C34-based peptides used in this study. The locations of the fusion peptide (FP), amino-terminal heptad region (N-HR), carboxyl-terminal heptad region (C-HR), transmembrane domain (TM), and C-HR-derived peptides are shown. The residue numbers of T-20 and C34 correspond to their positions in gp41. Substitutions of N- and C-HR in gp41 of wild-type (WT) and T-20_{S138A}-resistant HIV-1 are shown. Res.-WT and Res.-NDSA indicate resistant HIV-1 that were initially selected from wild-type and HIV-$1_{N43D/S138A}$, respectively. (B and C) Induction of T-20_{S138A}-resistant HIV-1 by dose-escalating selection in MT-2 cells. Induction of resistant HIV-1 was carried out for a total of 60 passages of HIV-1_{WT} (B) and HIV-$1_{N43D/S138A}$ (C), in 0.1 nM and 1 nM of T-20_{S138A}, respectively. At the indicated passages, proviral DNA was sequenced, and the EC_{50} values of the HIV-1 variants were determined using the MAGI assay. To improve the replication kinetics, substitution of D36G was introduced into the NL4-3 background used in this study (wild-type virus) (Izumi et al., 2009; Mink et al., 2005).

pH 7.4). CD spectra were recorded on an AVIV model 202 spectropolarimeter (Aviv Instruments, Proterion Corporation, Piscataway, NJ) with a 1 mm path-length cuvette at 25 °C as the average of eight scans. The thermal stability was assessed by monitoring the change in the CD signal at 222 nm. The midpoint of the thermal unfolding transition (melting temperature [T_m]) of each complex was determined as previously described (Izumi et al., 2009).

3. Results

3.1. Selection of HIV-1 resistant to T-20_{S138A}

An HIV-1_{NL4-3} strain containing a D36G substitution, which improves replication kinetics, was used as a wild-type virus (HIV-1_{WT}) and for the construction of various mutants, as described (Izumi et al., 2009; Mink et al., 2005). HIV-1_{WT} or T-20-resistant HIV-$1_{N43D/S138A}$ were used for selection of T-20_{S138A}-resistant HIV-1. MT-2 cells were infected with HIV-1_{WT} and HIV-$1_{N43D/S138A}$, and incubated in the presence of T-20_{S138A} at the initial concentrations of 0.1 nM and 1 nM, respectively. At the indicated passages, the sequence of the *env* region was determined by direct sequencing of the proviral DNA extracted from the infected MT-2 cells. During the selection, mutations in the gp41 were observed and are shown in Fig. 1B and C.

In the selection with HIV-1_{WT} (Fig. 1B), at passage 28 (P-28), when T-20_{S138A} concentration was 51.2 nM (P-28, 51.2 nM), isoleucine at position 37 in the gp41 was substituted to asparagine (I37N). At P-60 (3.3 μM), L44 M and N126K in the gp41 further emerged. On the other hand, in the selection with T-20-resistant HIV-$1_{N43D/S138A}$ (Fig. 1C), at P-28 (512 nM) and at P-40 (2 μM), E137K in the gp41, and L33S and I69L in the gp41 emerged, respectively. The emergence of the I69L mutation in diverse HIV-1 strains has been previously reported (Eshleman et al., 2007). At P-60, the resistance of selected viruses from HIV-1_{WT} and HIV-$1_{N43D/S138A}$ to T-20_{S138A}, reached approximately 110- and 200-fold, respectively. These results indicate that even though T-20_{S138A} was active against T-20 resistant variants, resistant HIV-1 emerged relatively rapidly compared with the next generation fusion inhibitors, such as SC34EK, which required 120 passages to acquire the resistance (Shimura et al., 2010).

3.2. Susceptibility of T-20_{S138A}-resistant HIV-1 to T-20 and C34 derivatives

To validate our resistance data we used site-directed mutagenesis to prepare recombinant HIV-1 with the T-20_{S138A}-resistance mutations and examined its susceptibility to T-20 and C34 derivatives with MAGI assay (Table 1). We also used as controls the modified α-helix T-20- and C34-peptide inhibitors, T-20EK (Oishi et al., 2008) and SC35EK (Nishikawa et al., 2009; Shimura et al., 2010), respectively, which are more efficient *in vitro* replication inhibitors of T-20-resistant HIV-1 than T-20 or C34. Finally, we also used as a control $C34_{N126K}$, a modified version of C34 that includes the resistance-associated N126K substitution that effectively suppress replication of C34-resistant HIV-1 *in vitro* (Izumi et al., 2009).

Selected mutations I37N and L33S provided various levels of resistance to T-20 and its derivatives, T-20_{S138A} and T-20EK, apparently acting as primary mutations to peptides with a T-20 backbone (Table 1). Other mutations, L44M, I69L, and E137K, which were

Table 1
Antiviral activity of C-HR-derived peptides against gp41 recombinant viruses.

	EC_{50} (nM)					
	T-20	T-20_{S138A}	T-20EK	C34	$C34_{N126K}$	SC35EK
HIV-1_{WT} [a]	2.4 ± 0.6	0.6 ± 0.1	1.9 ± 0.5	2.1 ± 0.7	1.6 ± 0.5	2.4 ± 0.9
HIV-1_{I37N}	47 ± 6.9 (**20**)	4.3 ± 1.3 (7.2)	21 ± 2.4 (**11**)	3.3 ± 1.1(1.6)	1.9 ± 0.1 (1.2)	1.0 ± 0.4(0.4)
HIV-1_{L44M}	4.1 ± 1.2 (1.7)	0.7 ± 0.2 (1.2)	2.2 ± 0.6 (1.2)	1.1 ± 0.3(0.5)	0.8 ± 0.2 (0.5)	0.6 ± 0.2(0.3)
HIV-1_{N126K}	4.4 ± 1.3 (1.8)	1.2 ± 0.4 (2.0)	2.8 ± 0.2 (1.5)	6.3 ± 1.2(3.0)	1.5 ± 0.2 (0.9)	3.3 ± 0.2(1.4)
HIV-$1_{I37N/N126K}$	660 ± 180(**275**)	16 ± 4.8 (**27**)	14 ± 5.1 (7.4)	20 ± 4.5(9.5)	3.4 ± 0.4 (2.1)	2.9 ± 0.3(1.2)
HIV-$1_{I37N/L44M/N126K}$	>1000 (>417)	130 ± 40(220)	240 ± 95(126)	66 ± 23 (31)	4.0 ± 0.8 (2.5)	1.1 ± 0.1(0.5)
HIV-1_{L33S}	23 ± 5.5 (9.6)	3.1 ± 0.6 (5.2)	13 ± 2.6 (6.8)	3.2 ± 1.1(1.5)	2.1 ± 0.1 (1.3)	3.0 ± 0.8(1.2)
HIV-1_{N43D}	49 ± 10 (**20**)	3.5 ± 0.9 (5.8)	4.1 ± 1.2 (2.2)	4.4 ± 0.4(2.1)	1.4 ± 0.1 (0.8)	0.4 ± 0.2(0.2)
HIV-1_{I69L}	2.1 ± 0.5 (0.9)	0.5 ± 0.2 (0.8)	2.2 ± 0.4 (1.2)	2.7 ± 0.2(1.3)	2.2 ± 0.5 (1.4)	2.7 ± 0.5(1.1)
HIV-1_{E137K}	2.0 ± 0.3 (0.8)	0.7 ± 0.1 (1.2)	2.5 ± 0.4 (1.3)	2.6 ± 0.2(1.2)	2.3 ± 0.7 (1.4)	3.1 ± 0.8(1.3)
HIV-$1_{N43D/S138A}$	84 ± 16 (**35**)	3.2 ± 1.0 (5.3)	3.4 ± 1.1 (1.8)	2.7 ± 0.2(1.3)	1.6 ± 0.5 (1.0)	0.3 ± 0.1(0.1)
HIV-$1_{L33S/N43D/S138A}$	>1000 (**>417**)	550 ± 72(**174**)	330 ± 94 (14)	30 ± 9.2(2.6)	4.2 ± 1.2 (0.4)	0.9 ± 0.3(0.4)
HIV-$1_{N43D/E137K/S138A}$	110 ± 31 (**46**)	14 ± 4.7 (**23**)	7.0 ± 2.4 (3.7)	7.4 ± 1.9(3.5)	2.1 ± 0.7 (1.3)	1.9 ± 0.6(0.8)
HIV-$1_{L33S/N43D/E137K/S138A}$	>1000 (**>417**)	>1000(**>1667**)	>1000 (**>526**)	31 ± 5.0 (**15**)	6.7 ± 1.7 (4.2)	1.2 ± 0.2(0.5)
HIV-$1_{L33S/N43D/I69L/E137K/S138A}$	>1000 (**>417**)	>1000(**>1667**)	>1000 (**>526**)	50 ± 12 (**24**)	28 ± 7.1(**17.5**)	1.0 ± 0.9(0.4)

Anti-HIV activity was determined using the MAGI assay. Fifty percent effective concentration (EC_{50}) values and SD were obtained from the results of at least three independent experiments. Shown in parentheses are the fold-increases in resistance (increase in EC_{50} value) calculated by comparison to a wild-type virus (HIV-1_{WT}). Increases of over 10-fold are indicated in bold.

[a] To improve the replication kinetics, substitution of D36G, observed in majority of HIV-1 strains, was introduced into the NL4-3 background used in this study (wild-type virus; HIV-1_{WT}) (Izumi et al., 2009; Mink et al., 2005).

observed in wild-type HIV-1 as polymorphisms (Kuiken et al., 2010; Loutfy et al., 2007), conferred little resistance to all peptide fusion inhibitors tested. However, introduction of L44M to HIV-$1_{I37N/N126K}$ (HIV-$1_{I37N/L44M/N126K}$) remarkably enhanced resistance to T-20 derivatives. This was consistent with previous studies that also reported a resistance enhancement (1.8-fold) by L44M to T-20 (Loutfy et al., 2007). Collectively, these data suggest that L44M has as a role in HIV-1 resistance as a secondary mutation. All peptides sufficiently suppressed HIV-1_{I69L}, suggesting that I69L may be a secondary mutation or a polymorphism. N126K conferred only marginal resistance (<3-fold) to all peptide fusion inhibitors, but in the background of I37N (HIV-$1_{I37N/N126K}$) it enhanced resistance to T-20, T-20_{S138A}, and C34. L33S, which was originally reported as a C34 resistance associated mutation (Armand-Ugon et al., 2003), significantly enhanced resistance in the background of N43D/S138A mutations (HIV-$1_{L33S/N43D/S138A}$). Similar to the N126K mutation, E137K also enhanced resistance by N43D/S138A (HIV-$1_{N43D/E137K/S138A}$) and L33S/N43D/S138A (HIV-$1_{L33S/N43D/E137K/S138A}$) to T-$20_{S138A}$, T-20, and T-20EK. These results indicate that L33S and I37N appear to be primary mutations for T-20 derivatives.

3.3. *Effect of substitutions in the gp120 on peptide susceptibility*

Polymorphisms in the gp120 that influence co-receptor usage may influence T-20 susceptibility (Labrosse et al., 2003; Reeves et al., 2002). Meanwhile, others reported that T-20 susceptibility was not influenced by co-receptor usage (Cilliers et al., 2004; Melby et al., 2006). Resistance induction experiments performed in this study revealed that most laboratory strains with *in vitro* resistance to fusion inhibitors acquired substitutions in both the gp120 and the gp41 (Armand-Ugon et al., 2003; Eggink et al., 2011; Fikkert et al., 2002; Izumi et al., 2010; Nameki et al., 2005; Shimura et al., 2010). However, most substitutions showed little impact on resistance, and only contributed to a small enhancement of replication capacity (Eggink et al., 2011; Izumi et al., 2010; Nameki et al., 2005; Shimura et al., 2010). In the present study, we examined peptide susceptibility of cloned viruses that contain all Env substitutions observed in the selection (both gp120 and gp41). Most substitutions in the gp120 attenuated resistance to fusion inhibitors (Table 3). Therefore, *in vitro* experiments showed that substitutions in the gp120 are not likely associated with resistance.

3.4. *Influence of mutations in the gp41 on HIV-1 replication*

To address the effects of mutations on HIV-1 replication, we examined the replication kinetics of T-20_{S138A}-resistant HIV-$1_{N43D/S138A}$ variants. Consistent with a previous report (Lohrengel et al., 2005), the L33S mutation did not significantly affect the replication kinetics and infectivity compared with those of HIV-1_{WT} (Fig. 2A). The S138A mutation restored the replication

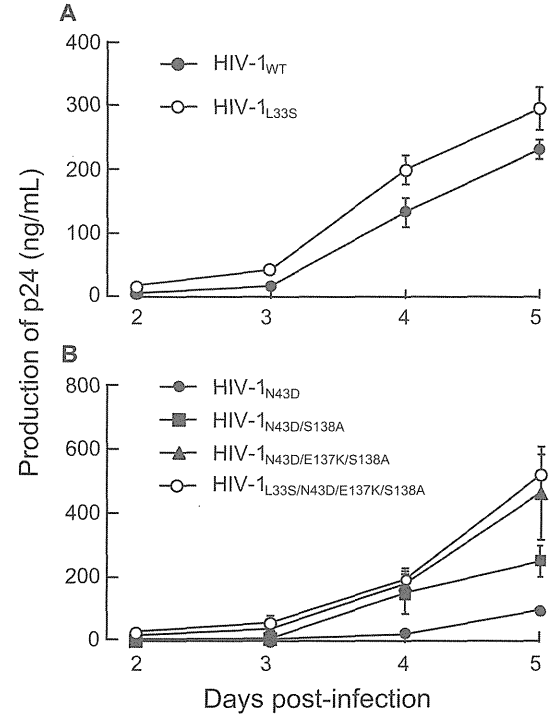

Fig. 2. Replication kinetics of T-20_{S138A}-resistant variants. Replication kinetics of T-20_{S138A}-resistant recombinant variants that introduced L33S mutation (A), or combinations of L33S, E137K, and S138A mutations in HIV-1_{N43D} (B). To improve replication kinetics, the D36G polymorphism was introduced into the NL4-3 background used in this study (HIV-1_{WT}). Supernatants from infected MT-2 cells were collected on days 2–7 and the amount of p24 produced was determined. Representative results are shown as mean values with standard deviations estimated from three independent experiments.

kinetics of HIV-1_{N43D} (Fig. 2B), as previously described (Izumi et al., 2009). E137K was also associated with N43D mutation *in vivo* (Svicher et al., 2008), and restored infectivity impaired by N43D (Tolstrup et al., 2007). Introduction of E137K into N43D/S138A enhanced the replication kinetics, and further addition of L33S to N43D/E137K/S138A resulted in equivalent replication kinetics compared with HIV-$1_{N43D/E137K/S138A}$ (Fig. 2B) as observed in HIV-1_{WT} based mutants. During the passage of HIV-$1_{N43D/S138A}$, a synonymous mutation at amino acid position L44, TTG to CTG, was observed. Interestingly, $L_{TTG}44L_{CTG}$ enhanced viral replication kinetics through enhanced stability of the Rev-responsive element (RRE) secondary structure (Ueno et al., 2009). Therefore, we examined the viral replication kinetics of mutants with $L_{TTG}44L_{CTG}$, and compared HIV-1_{WT}, with HIV-$1_{L44L\text{-}CTG}$, and HIV-$1_{L33S/N43D/L44L\text{-}CTG/E137K/S138A}$ with HIV-$1_{L33S/N43D/L44L\text{-}CTG/I69L/E137K/S138A}$. As expected, the presence of $L_{TTG}44L_{CTG}$ enhanced replication in all viruses. Surprisingly, mutants with resistance mutations showed enhanced replication kinetics as determined by the p24 production assay of culture supernatants (Fig. 4A). Therefore, we further examined infectivity using the MAGI assay and determined that the infectivity of resistance variants containing $L_{TTG}44L_{CTG}$ was reduced compared with HIV-1_{WT} (Fig. 4B). These results indicate that the primary mutation, L33S, possesses less ability to attenuate HIV-1 replication, while I69L, S138A, and E137K enhance replication kinetics of T-20-resistant HIV-1 to a comparable level of HIV-1_{WT}.

3.5. Circular dichroism

To clarify the effect of E137K substitutions on peptide binding, we examined the binding affinities of E137K-containing C-HR peptides to N-HR using CD analysis. CD spectra reveal the presence of stable α-helical structures of six-helix bundles that are required for biological activity and are thought to mechanistically and thermodynamically correlate with HIV-1 fusion (Bianchi et al., 2005). Since *in vitro* T-20 does not interact with the N36 peptide (amino acid positions 35–70 of the N-HR), we used instead peptide C34 with E137K and/or S138A substitutions (Fig. 1A). We found that mixtures of $C34_{E137K}$, $C34_{S138A}$, or $C34_{E137K/S138A}$ with N36 or $N36_{N43D}$ showed sufficient and comparable α-helicity at 25 °C (Fig. 3A and B). We also determined the thermal stability of the helical complexes formed by the N36 and C34 peptides, which is also an indication of the binding affinity of these peptides. Hence, we measured and compared the melting temperatures (T_m) of various complexes, which indicates the 50% disruption of the six-helix bundle (Fig. 3C). Complexes of N36 and C34 containing the S138A and E137K/S138A substitutions (N36/$C34_{S138A}$ and N36/$C34_{E137K/S138A}$, respectively), showed higher thermal stability than N36/C34. Similarly, S138A and E137K/S138A restored the binding affinity of C34 to $N36_{N43D}$. These results indicate that E137K acts as a compensatory mutation for the T-20_{S138A}-resistance primary mutation, causing enhancement of replication kinetics.

3.6. Antiviral activity of E137K-modified peptides

Recently, we demonstrated that introduction of the S138A secondary mutation to T-20 (T-20_{S138A}) enhanced binding to mutated N-HR and suppresses resistance of T-20-resistance variants (Izumi et al., 2009). Similarly, as shown in Fig. 3, E137K enhanced binding affinity with N-HR, suggesting that introduction of E137K to T-20 may enhance the antiviral activity of T-20. We synthesized T-20 and T-20_{S138A} variants containing the E137K change (T-20_{E137K} and T-$20_{E137K/S138A}$) (Fig. 1A) and examined their anti-HIV activity against T-20_{S138A}-resistant HIV-1 (Table 2). All peptides exhibited potent antiviral activity against HIV-1_{WT}. HIV-$1_{L33S/N43D/S138A}$ and HIV-$1_{I37N/L44M/N126K}$ showed high resistance to T-20_{E137K},

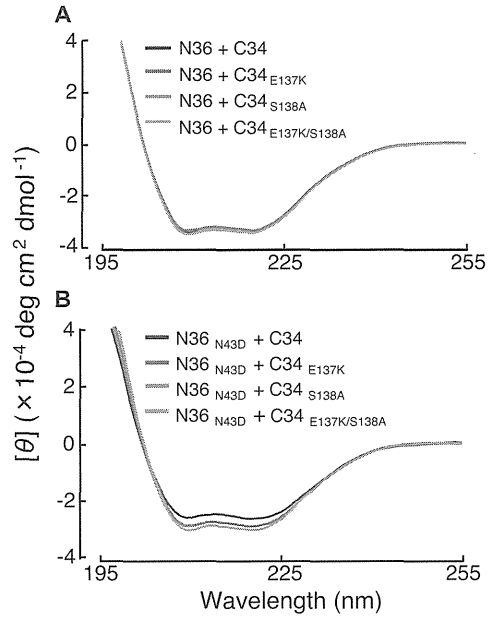

C

	T_m (°C)	
	N36	$N36_{N43D}$
C34	67.6	53.2
$C34_{E137K}$	68.9	56.7
$C34_{S138A}$	73.2	58.0
$C34_{E137K/S138A}$	74.6	63.3

Fig. 3. CD spectra (A and B) and thermal stability (C) of N36/C34 complexes. Peptide sequences used in this study are shown in FIG 1A and have also been previously described (Izumi et al., 2009). CD spectra of $C34_{E137K}$, $C34_{S138A}$, and $C34_{E137K/S138A}$ complexes with N36 (A) and $N36_{N43D}$ (B) are shown. Equimolar amounts (10 μM) of the N- and C-HR peptides were incubated at 37 °C for 30 min in PBS. The CD spectra of each mixture were then collected at 25 °C using a Jasco (Model J-710) spectropolarimeter. (C) Thermal stabilities, defined as the midpoint of the thermal unfolding transition (T_m) values, of the potential six-helix bundles of N- and C-HR peptides, were determined.

indicating that the resistance mechanism of T-20_{E137K} is similar to that of T-20_{S138A}. On the other hand, T-$20_{E137K/S138A}$ (Table 2) maintained some antiviral activity against HIV-$1_{L33S/N43D/S138A}$, HIV-$1_{L33S/N43D/E137K/S138A}$, and HIV-$1_{I37N/L44M/N126K}$ compared with other T-20 derivatives including electrostatically constrained T-20EK (Table 1 and Fig. 1). $C34_{E137K}$ and $C34_{E137K/S138A}$ significantly suppressed all HIV-1 variants tested except for HIV-$1_{I37N/L44M/N126K}$ by $C34_{E137K}$. These results indicate that peptides with resistant mutations may sustain their activity against particular resistant variants.

4. Discussion

The current study describes the introduction of resistance changes into the original and modified (T-20_{S138A}) versions of the T-20 peptide-fusion inhibitor. We analyzed the new T-20 derivatives using both wild-type and T-20-resistant strains. We also identified through dose escalation experiments, T-20_{S138A}-resistants. We found that T-20_{S138A}-resistant HIV-1 showed cross-resistance only to the T-20 derivatives, but not to C34 derivatives. Through the CD analysis, the N126K and E137K mutations in the C-HR may act as compensatory mutations for impaired interaction by a primary mutation, I37N and N43D in the N-HR, respectively. Since E137K is located within the T-20 sequence, we synthesized and characterized the activity of novel T-20-based peptides containing E137K (T-20_{E137K}). Here we demonstrate that

Table 2
Antiviral activity of E137K-induced C-HR peptides against T-20_{S138A}-resistant variants.

	EC_{50} (nM)			
	T-20_{E137K}	T-$20_{E137K/S138A}$	$C34_{E137K}$	$C34_{E137K/S138A}$
HIV-1_{WT} [a]	0.8 ± 0.2	0.5 ± 0.1	1.0 ± 0.3	0.7 ± 0.2
HIV-1_{L33S}	13 ± 3.2 (**16**)	2.2 ± 0.4 (4.5)	0.7 ± 0.2(0.7)	0.5 ± 0.1(0.7)
HIV-$1_{N43D/S138A}$	4.2 ± 0.7 (5.3)	0.7 ± 0.2 (1.4)	0.3 ± 0.1(0.3)	0.4 ± 0.1(0.6)
HIV-$1_{L33S/N43D/S138A}$	700 ± 150 (**880**)	45 ± 9.9 (**90**)	2.3 ± 0.4(2.3)	0.5 ± 0.2(0.7)
HIV-$1_{N43D/E137K/S138A}$	12 ± 3.6 (**15**)	2.4 ± 0.8 (4.8)	0.2 ± 0.1(0.2)	0.4 ± 0.1(0.6)
HIV-$1_{L33S/N43D/E137K/S138A}$	480 ± 47 (**600**)	36 ± 3.1 (**72**)	3.8 ± 1.3(3.8)	1.0 ± 0.4(1.4)
HIV-$1_{L33S/N43D/I69L/E137K/S138A}$	1808 ± 852(2260)	157 ± 83(314)	4 ± 2 (4)	1.0 ± 0.4(1.4)
HIV-$1_{I37N/L44M/N126K}$	200 ± 24 (**250**)	30 ± 8.7 (**60**)	17 ± 3.8 (**17**)	2.2 ± 0.3(3.1)

Anti-HIV activity was determined using the MAGI assay. Fifty percent effective concentration (EC_{50}) values and SD were obtained from the results of at least three independent experiments. Shown in parentheses are the fold-increases in resistance (increase in EC_{50} value) calculated by comparison to a wild-type virus (HIV-1_{WT}). Increases of over 10-fold are indicated in bold.

[a] To improve the replication kinetics, substitution of D36G, observed in majority of HIV-1 strains, was introduced into the NL4-3 background used in this study (wild-type virus; HIV-1_{WT}) (Izumi et al., 2009; Mink et al., 2005).

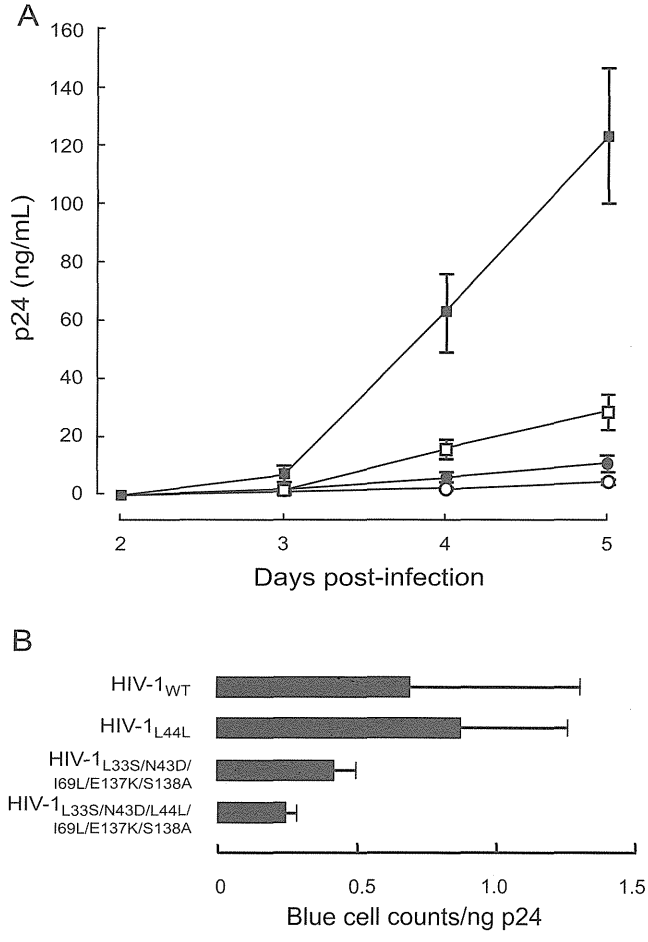

Fig. 4. Effect of secondary mutations in the N-HR on (A) replication kinetics and (B) infectivity. $L_{TTG}44L_{CTG}$ was introduced into HIV-1_{WT} and T-20_{S138A} resistant HIV-1 (HIV-$1_{L33S/N43D/L44L\text{-}CTG/I69L/E137K/S138A}$). Replication kinetics were determined by measuring p24 production in culture supernatants. HIV-1_{WT} (open circles), HIV-1_{L44L} (closed circles) HIV-$1_{L33S/N43D/I69L/E137K/S138A}$ (open squares), and HIV-$1_{L33S/N43D/L44L\text{-}CTG/I69L/E137K/S138A}$ (closed squares). $L_{TTG}44L_{CTG}$ introduction statistically enhanced both replication of HIV-1_{WT} and HIV-$1_{L33S/N43D/L44L\text{-}CTG/I69L/E137K/S138A}$ (Student's *t*-test, $p < 0.01$ on day 4 and 5). Relative infectivity (blue cell counts in MAGI cells divided by amount of p24) was calculated (B). Error bars indicate SD of three determinations. Decrease of infectivity between HIV-$1_{L33S/N43D/I69L/E137K/S138A}$ and HIV-$1_{L33S/N43D/L44L\text{-}CTG/I69L/E137K/S138A}$ were statistically significant (Student's *t*-test, $p < 0.05$).

the introduction of a secondary resistance mutation (E137K) in the backbone of a peptide fusion inhibitor is a useful change that results into more potent fusion inhibitors, even for HIV-1 strains that are resistant to peptide fusion inhibitors.

Selection of T-20_{S138A}-resistance starting with wild-type HIV-1 resulted in the emergence of I37N and L44M substitutions, which were located in the N-HR region that is thought to interact with T-20. Other substitutions at position 37 (I37T or I37K) also conferred resistance to T-20 and C34 (Nameki et al., 2005), suggesting that I37 in N-HR is critical for the attachment of C-HR-derived peptide fusion inhibitors. The L44M mutation has only been observed in subtype B HIV-1-infected patients treated with T-20 (Carmona et al., 2005), and conferred weak resistance to T-20 (Loutfy et al., 2007). In this study, L44M did not confer resistance to all peptide inhibitors; however, L44M in combination with other mutations (I37N/N126K) remarkably enhanced resistance to T-20_{S138A}, suggesting that L44M serves as a secondary mutation to enhance resistance to T-20_{S138A}. N126K also enhances resistance to some fusion inhibitors (Baldwin et al., 2004; Nameki et al., 2005; Eggink et al., 2008) by helping recover losses in intra-gp41 interactions that were caused by primary mutations, such as N43D.

When we selected T-20_{S138A}-resistant HIV-1 (HIV-$1_{N43D/S138A}$) we obtained a somehow different set of mutations that included L33S, which is located at the presumed T-20 binding site at N-HR, as well as I37N, N43D, and L44M. L33S was previously reported in HIV-1 variants resistant to T-20 (Fikkert et al., 2002), C34 (Armand-Ugon

Table 3
Antiviral activity of C-HR-derived peptides against gp160 recombinant viruses.

Compound	EC_{50} (nM)	
ddC	771 ± 272	
T-20 derivatives		
T20	>10,000	(NA)
T20EK	2729 ± 1113	(NA)
$T20_{S138A}$	3126 ± 453	(NA)
$T20_{E137K}$	2761 ± 1477	(NA)
$T20_{E137K/S138A}$	203 ± 54	(0.6)
C34 derivatives		
C34	171.0 ± 106	(3.4)
$C34_{N126K}$	25.9 ± 4.6	(NA)
SC34EK	1.0 ± 0.8	(1)
$C34_{E137K}$	7.0 ± 4.4	(0.4)
$C34_{E137K/S138A}$	0.3 ± 0.1	(0.3)

Anti-HIV activity was determined using the MAGI assay. Fifty percent effective concentration (EC_{50}) values and SD were obtained from the results of at least three independent experiments. Shown in parentheses are the fold-increases in resistance (increase in EC_{50} value) calculated by comparison to the resistant clone with mutations only in gp41 (HIV-$1_{L33S/N43D/I69L/E137K/S138A}$). To improve the replication kinetics, substitution of D36G, observed in majority of HIV-1 strains, was introduced into the NL4-3 background used in this study (Izumi et al., 2009; Mink et al., 2005). NA, not available; ddC, dideoxycytidine.

et al., 2003), and a membrane-anchored C-HR-derived peptide, M87 (Lohrengel et al., 2005). Although our work clearly demonstrates that L33S is involved in resistance to T-20 derivatives, it was not possible to discern whether L33S affected binding affinity to C-HR in the CD analyses because L33 was not in the sequence of the N36 N-HR peptide that we had to use in this study. As shown in Fig. 2, L33S did not significantly affect replication kinetics compared with HIV-1_{WT}, suggesting that L33S might sustain binding affinity with C-HR to form a stable six-helix bundle. The L33S mutation is located in the loop of stem IIc of the RRE (Ueno et al., 2009). Hence, nucleotide changes for L33S do not require compensatory mutations to maintain secondary structure of the RRE. Therefore, it is likely that L33S has little effect on replication kinetics. In this study, L33S conferred little resistance to C34 in this study, while it was previously reported to confer up to 10-fold resistance (Armand-Ugon et al., 2003), suggesting that some other viral background might affect the resistance, since Armand-Ugon et al. (2003) examined bulk virus samples obtained from the selection.

A prevalent polymorphism, E137K, which was associated with N43D *in vivo* (Svicher et al., 2008), has been proven to restore infectivity that has been impaired by N43D (Tolstrup et al., 2007). E137K did not affect susceptibility to all peptide fusion inhibitors by itself, but in combination with primary mutations, it remarkably enhanced resistance to T-20_{S138A}. Moreover, introduction of the E137K change into N43D/S138A enhanced the viral replication kinetics as shown in Fig. 2. A possible hydrogen bond between K137 and D43 may partially restore the reported loss in six-helix bundle stability conferred by the N43D mutation (Bai et al., 2008), suggesting that E137K can compensate for losses in the interactions between N-HR_{N43D} and C-HR. This hypothesis is consistent with our CD results presented in Fig. 3.

Because E137K restored binding affinity with N-HR similar to the S138A mutation, we expected that introduction of E137K into T-20 would effectively suppresses replication of T-20-resistant HIV-1. We examined the antiviral activity of E137K- and E137K/S138A-containing T-20 and C34 to T-20_{S138A}-resistant HIV-1. We found that T-20_{E137K} had similar antiviral activity with other T-20 derivatives such as T-20_{S138A} and T-$20_{E137K/S138A}$. Hence, we believe that the combination of few substitution secondary mutations can enhance the antiviral activity of peptide fusion inhibitors. Therefore, it is possible to design peptides that include the secondary mutations in the C-HR and use them by themselves and/or in combinations to block fusion inhibitor resistant viruses. Importantly, we have successfully applied this strategy to suppress HIV-1 resistance to next generation fusion inhibitor SC34EK (Shimura et al., 2010).

In this study, we identified two distinct pathways to escape pressure of T-20_{S138A}. Emergence of drug resistance mutants under drug pressure involves a stochastic selection. Nonetheless, the makeup of the final population depends on both the ability of specific populations to evade the drug, as well as their fitness that determines their representation in the escape population. There are several examples in the literature where HIV becomes resistant to the same drug by different mechanisms. For example, in the case of the most commonly used drugs that target HIV reverse transcriptase (RT), the virus can develop multidrug resistance by either the Q151M complex pathway (Kavlick et al., 1998; Shirasaka et al., 1995) or by accumulation of thymidine associated mutations (TAMs) (Hachiya et al., 2008; Kosalaraksa et al., 1999). We recently report some of background polymorphisms can also influence resistance pathways, such 172R/K in the RT region (Hachiya et al., 2012). In the case of the T-20S138A inhibitor, the N43D/S138A may also act as such polymorphisms despite the presence of primary mutations (Izumi et al., 2009) and preferentially affect the emergence of specific mutations.

5. Conclusion

As previously discussed (Izumi et al., 2009), although other developed peptide-based fusion inhibitors need many amino acid additions and/or substitutions for the enhancement of their antiviral activity (Chinnadurai et al., 2007; Eggink et al., 2008; Dwyer et al., 2007; Otaka et al., 2002), application of secondary mutations similar to T-20_{S138A} and T-$20_{E137K/S138A}$ is straightforward. It is based on information from viral evolution studies under drug pressure that help design improved inhibitors.

Acknowledgments

This work was supported by a grant from the Ministry of Education, Culture, Sports, Science, and Technology of Japan, a grant for the Promotion of AIDS Research from the Ministry of Health, Labour and Welfare. Additional support was by National Institute of Health (NIH) research Grants AI094715, AI076119, AI079801, and AI100890 (SGS). We are grateful to Biomedical Research Core (Tohoku University School of Medicine) for technical support. The authors declare non-financial competing interests.

References

Aquaro S, D'Arrigo R, Svicher V, Perri GD, Caputo SL, Visco-Comandini U, et al. Specific mutations in HIV-1 gp41 are associated with immunological success in HIV-1-infected patients receiving enfuvirtide treatment. Journal of Antimicrobial Chemotherapy 2006;58:714–22.

Armand-Ugon M, Gutierrez A, Clotet B, Este JA. HIV-1 resistance to the gp41-dependent fusion inhibitor C-34. Antiviral Research 2003;59:137–42.

Bai X, Wilson KL, Seedorff JE, Ahrens D, Green J, Davison DK, et al. Impact of the enfuvirtide resistance mutation N43D and the associated baseline polymorphism E137K on peptide sensitivity and six-helix bundle structure. Biochemistry 2008;47:6662–70.

Baldwin CE, Sanders RW, Deng Y, Jurriaans S, Lange JM, Lu M, et al. Emergence of a drug-dependent human immunodeficiency virus type 1 variant during therapy with the T20 fusion inhibitor. Journal of Virology 2004;78:12428–37.

Bianchi E, Finotto M, Ingallinella P, Hrin R, Carella AV, Hou XS, et al. Covalent stabilization of coiled coils of the HIV gp41N region yields extremely potent and broad inhibitors of viral infection. Proceedings of the National Academy of Sciences of the United States of America 2005;102:12903–8.

Cabrera C, Marfil S, Garcia E, Martinez-Picado J, Bonjoch A, Bofill M, et al. Genetic evolution of gp41 reveals a highly exclusive relationship between codons 36, 38 and 43 in gp41 under long-term enfuvirtide-containing salvage regimen. AIDS 2006;20:2075–80.

Cardoso RM, Brunel FM, Ferguson S, Zwick M, Burton DR, Dawson PE, et al. Structural basis of enhanced binding of extended and helically constrained peptide epitopes of the broadly neutralizing HIV-1 antibody 4E10. Journal of Molecular Biology 2007;365:1533–44.

Carmona R, Perez-Alvarez L, Munoz M, Casado G, Delgado E, Sierra M, et al. Natural resistance-associated mutations to enfuvirtide (T20) and polymorphisms in the gp41 region of different HIV-1 genetic forms from T20 naive patients. Journal of Clinical Virology 2005;32:248–53.

Chan DC, Chutkowski CT, Kim PS. Evidence that a prominent cavity in the coiled coil of HIV type 1 gp41 is an attractive drug target. Proceedings of the National Academy of Sciences of the United States of America 1998;95:15613–7.

Chan DC, Fass D, Berger JM, Kim PS. Core structure of gp41 from the HIV envelope glycoprotein. Cell 1997;89:263–73.

Chinnadurai R, Rajan D, Munch J, Kirchhoff F. Human immunodeficiency virus type 1 variants resistant to first- and second-version fusion inhibitors and cytopathic in ex vivo human lymphoid tissue. Journal of Virology 2007;81:6563–72.

Cilliers T, Patience T, Pillay C, Papathanasopoulos M, Morris L. Sensitivity of HIV type 1 subtype C isolates to the entry inhibitor T-20. AIDS Research and Human Retroviruses 2004;20:477–82.

Debnath AK, Radigan L, Jiang S. Structure-based identification of small molecule antiviral compounds targeted to the gp41 core structure of the human immunodeficiency virus type 1. Journal of Medicinal Chemistry 1999;42:3203–9.

Dwyer JJ, Wilson KL, Davison DK, Freel SA, Seedorff JE, Wring SA, et al. Design of helical, oligomeric HIV-1 fusion inhibitor peptides with potent activity against enfuvirtide-resistant virus. Proceedings of the National Academy of Sciences of the United States of America 2007;104:12772–7.

Dwyer JJ, Wilson KL, Martin K, Seedorff JE, Hasan A, Medinas RJ, et al. Design of an engineered N-terminal HIV-1 gp41 trimer with enhanced stability and potency. Protein Science 2008;17:633–43.

Eggink D, Baldwin CE, Deng Y, Langedijk JP, Lu M, Sanders RW, et al. Selection of T1249-resistant human immunodeficiency virus type 1 variants. Journal of Virology 2008;82:6678–88.

Eggink D, Bontjer I, Langedijk JP, Berkhout B, Sanders RW. Resistance of human immunodeficiency virus type 1 to a third-generation fusion inhibitor requires

multiple mutations in gp41 and is accompanied by a dramatic loss of gp41 function. Journal of Virology 2011;85:10785–97.
Eshleman SH, Hudelson SE, Bruce R, Lee T, Owens MR, Hackett J, et al. Analysis of HIV type 1 gp41 sequences in diverse HIV type 1 strains. AIDS Research and Human Retroviruses 2007;23:1593–8.
Fikkert V, Cherepanov P, Van Laethem K, Hantson A, Van Remoortel B, Pannecouque C, et al. env chimeric virus technology for evaluating human immunodeficiency virus susceptibility to entry inhibitors. Antimicrobial Agents and Chemotherapy 2002;46:3954–62.
Hachiya A, Kodama EN, Sarafianos SG, Schuckmann MM, Sakagami Y, Matsuoka M, Takiguchi M, Gatanaga H, Oka S. Amino acid mutation N348I in the connection subdomain of human immunodeficiency virus type 1 reverse transcriptase confers multiclass resistance to nucleoside and nonnucleoside reverse transcriptase inhibitors. Jouranl of Virology 2008;82:3261–70.
Hachiya A, Marchand B, Kirby KA, Michailidis E, Tu X, Palczewski K, Ong YT, Li Z, Griffin DT, Schuckmann MM, Tanuma J, Oka S, Singh K, Kodama EN, Sarafianos SG. HIV-1 reverse transcriptase (RT) polymorphism 172K suppresses the effect of clinically relevant drug resistance mutations to both nucleoside and nonnucleoside RT inhibitors. Journal of Biological Chemistry 2012;287:29988–99.
He Y, Xiao Y, Song H, Liang Q, Ju D, Chen X, et al. Design and evaluation of sifuvirtide, a novel HIV-1 fusion inhibitor. Journal of Biological Chemistry 2008;283:11126–34.
Izumi K, Kodama E, Shimura K, Sakagami Y, Watanabe K, Ito S, et al. Design of peptide-based inhibitors for human immunodeficiency virus type 1 strains resistant to T-20. Journal of Biological Chemistry 2009;284:4914–20.
Izumi K, Nakamura S, Nakano H, Shimura K, Sakagami Y, Oishi S, et al. Characterization of HIV-1 resistance to a fusion inhibitor, N36, derived from the gp41 amino-terminal heptad repeat. Antiviral Research 2010;87:179–86.
Kavlick MF, Wyvill K, Yarchoan R, Mitsuya H. Emergence of multidideoxynucleoside-resistant human immunodeficiency virus type 1 variants, viral sequence variation, and disease progression in patients receiving antiretroviral chemotherapy. Journal of Infectious Diseases 1998;177:1506–13.
Kilby JM, Hopkins S, Venetta TM, DiMassimo B, Cloud GA, Lee JY, et al. Potent suppression of HIV-1 replication in humans by T-20, a peptide inhibitor of gp41-mediated virus entry. Nature Medicine 1998;4:1302–7.
Kosalaraksa P, Kavlick MF, Maroun V, Le R, Mitsuya H. Comparative fitness of multi-dideoxynucleoside-resistant human immunodeficiency virus type 1 (HIV-1) in an In vitro competitive HIV-1 replication assay. Jouranl of Virology 1999;73:5356–63.
Kuiken C, Foley B, Leitner T, Apetrei C, Hahn B, Mizrachi I, et al. HIV sequence compendium 2010. Los Alamos, NM: Los Alamos National Laboratory, Theoretical Biology and Biophysics; 2010.
Labrosse B, Labernardiere JL, Dam E, Trouplin V, Skrabal K, Clavel F, et al. Baseline susceptibility of primary human immunodeficiency virus type 1 to entry inhibitors. Journal of Virology 2003;77:1610–3.
Lalezari JP, Henry K, O'Hearn M, Montaner JS, Piliero PJ, Trottier B, et al. Enfuvirtide, an HIV-1 fusion inhibitor, for drug-resistant HIV infection in North and South America. New England Journal of Medicine 2003;348:2175–85.
Lazzarin A, Clotet B, Cooper D, Reynes J, Arasteh K, Nelson M, et al. Efficacy of enfuvirtide in patients infected with drug-resistant HIV-1 in Europe and Australia. New England Journal of Medicine 2003;348:2186–95.
Lohrengel S, Hermann F, Hagmann I, Oberwinkler H, Scrivano L, Hoffmann C, et al. Determinants of human immunodeficiency virus type 1 resistance to membrane-anchored gp41-derived peptides. Journal of Virology 2005;79:10237–46.
Loutfy MR, Raboud JM, Montaner JS, Antoniou T, Wynhoven B, Smaill F, et al. Assay of HIV gp41 amino acid sequence to identify baseline variation and mutation development in patients with virologic failure on enfuvirtide. Antiviral Research 2007;75:58–63.
Malashkevich VN, Chan DC, Chutkowski CT, Kim PS. Crystal structure of the simian immunodeficiency virus (SIV) gp41 core: conserved helical interactions underlie the broad inhibitory activity of gp41 peptides. Proceedings of the National Academy of Sciences of the United States of America 1998;95:9134–9.
Melby T, Sista P, DeMasi R, Kirkland T, Roberts N, Salgo M, et al. Characterization of envelope glycoprotein gp41 genotype and phenotypic susceptibility to enfuvirtide at baseline and on treatment in the phase III clinical trials TORO-1 and TORO-2. AIDS Research and Human Retroviruses 2006;22:375–85.
Mink M, Mosier SM, Janumpalli S, Davison D, Jin L, Melby T, et al. Impact of human immunodeficiency virus type 1 gp41 amino acid substitutions selected during enfuvirtide treatment on gp41 binding and antiviral potency of enfuvirtide in vitro. Journal of Virology 2005;79:12447–54.
Nameki D, Kodama E, Ikeuchi M, Mabuchi N, Otaka A, Tamamura H, et al. Mutations conferring resistance to human immunodeficiency virus type 1 fusion inhibitors are restricted by gp41 and Rev-responsive element functions. Journal of Virology 2005;79:764–70.
Nishikawa H, Nakamura S, Kodama E, Ito S, Kajiwara K, Izumi K, et al. Electrostatically constrained alpha-helical peptide inhibits replication of HIV-1 resistant to enfuvirtide. International Journal of Biochemistry and Cell Biology 2009;41:891–9.
Oishi S, Ito S, Nishikawa H, Watanabe K, Tanaka M, Ohno H, et al. Design of a novel HIV-1 fusion inhibitor that displays a minimal interface for binding affinity. Journal of Medicinal Chemistry 2008;51:388–91.
Oliveira AC, Martins AN, Pires AF, Arruda MB, Tanuri A, Pereira HS, et al. Enfuvirtide (T-20) resistance-related mutations in HIV type 1 subtypes B, C, and F isolates from Brazilian patients failing HAART. AIDS Research and Human Retroviruses 2009;25:193–8.
Otaka A, Nakamura M, Nameki D, Kodama E, Uchiyama S, Nakamura S, et al. Remodeling of gp41-C34 peptide leads to highly effective inhibitors of the fusion of HIV-1 with target cells. Angewandte Chemie International Edition in English 2002;41:2937–40.
Reeves JD, Gallo SA, Ahmad N, Miamidian JL, Harvey PE, Sharron M, et al. Sensitivity of HIV-1 to entry inhibitors correlates with envelope/coreceptor affinity, receptor density, and fusion kinetics. Proceedings of the National Academy of Sciences of the United States of America 2002;99:16249–54.
Shimura K, Nameki D, Kajiwara K, Watanabe K, Sakagami Y, Oishi S, et al. Resistance profiles of novel electrostatically constrained HIV-1 fusion inhibitors. Journal of Biological Chemistry 2010;285:39471–80.
Shirasaka T, Kavlick MF, Ueno T, Gao WY, Kojima E, Alcaide ML, Chokekijchai S, Roy BM, Arnold E, Yarchoan R, et al. Emergence of human immunodeficiency virus type 1 variants with resistance to multiple dideoxynucleosides in patients receiving therapy with dideoxynucleosides. Proceedings of the National Academy of Sciences of the United States of America 1995;92:2398–402.
Svicher V, Aquaro S, D'Arrigo R, Artese A, Dimonte S, Alcaro S, et al. Specific enfuvirtide-associated mutational pathways in HIV-1 Gp41 are significantly correlated with an increase in CD4(+) cell count, despite virological failure. Journal of Infectious Diseases 2008;197:1408–18.
Tolstrup M, Selzer-Plon J, Laursen AL, Bertelsen L, Gerstoft J, Duch M, et al. Full fusion competence rescue of the enfuvirtide resistant HIV-1 gp41 genotype (43D) by a prevalent polymorphism (137 K). AIDS 2007;21:519–21.
Ueno M, Kodama EN, Shimura K, Sakurai Y, Kajiwara K, Sakagami Y, et al. Synonymous mutations in stem-loop III of Rev responsive elements enhance HIV-1 replication impaired by primary mutations for resistance to enfuvirtide. Antiviral Research 2009;82:67–72.
Watabe T, Terakawa Y, Watanabe K, Ohno H, Nakano H, Nakatsu T, et al. X-ray crystallographic study of an HIV-1 fusion inhibitor with the gp41 S138A substitution. Journal of Molecular Biology 2009;392:657–65.
Welch BD, VanDemark AP, Heroux A, Hill CP, Kay MS. Potent D-peptide inhibitors of HIV-1 entry. Proceedings of the National Academy of Sciences of the United States of America 2007;104:16828–33.
Xu L, Pozniak A, Wildfire A, Stanfield-Oakley SA, Mosier SM, Ratcliffe D, et al. Emergence and evolution of enfuvirtide resistance following long-term therapy involves heptad repeat 2 mutations within gp41. Antimicrobial Agents and Chemotherapy 2005;49:1113–9.

«paper no. vir047167 charlesworth ref: vir047167»

Animal - RNA viruses

Journal of General Virology (2013), 94, 000–000 DOI 10.1099/vir.0.047167-0

Impact of antiretroviral pressure on selection of primary human immunodeficiency virus type 1 envelope sequences *in vitro*

Shigeyoshi Harada,[1,2] Kazuhisa Yoshimura,[1,2] Aki Yamaguchi,[1] Samatchaya Boonchawalit,[1,2] Keisuke Yusa[3] and Shuzo Matsushita[1]

Correspondence
Kazuhisa Yoshimura
ykazu@nih.go.jp

[1]Center for AIDS Research, Kumamoto University, 2-2-1 Honjo, Kumamoto 860-0811, Japan

[2]AIDS Research Center, National Institute of Infectious Diseases, 1-23-1 Toyama, Shinjuku-ku, Tokyo 162-8640, Japan

[3]Division of Biological Chemistry and Biologicals, National Institute of Health Sciences, 1-18-1 Kami-youga, Setagaya-ku, Tokyo 158-8501, Japan

The initiation of drug therapy results in a reduction in the human immunodeficiency virus type 1 (HIV-1) population, which represents a potential genetic bottleneck. The effect of this drug-induced genetic bottleneck on the population dynamics of the envelope (Env) regions has been addressed in several *in vivo* studies. However, it is difficult to investigate the effect on the *env* gene of the genetic bottleneck induced not only by entry inhibitors but also by non-entry inhibitors, particularly *in vivo*. Therefore, this study used an *in vitro* selection system using unique bulk primary isolates established in the laboratory to observe the effects of the antiretroviral drug-induced bottleneck on the integrase and *env* genes. Env diversity was decreased significantly in one primary isolate [KP-1, harbouring both CXCR4 (X4)- and CCR5 (R5)-tropic variants] when passaged in the presence or absence of raltegravir (RAL) during *in vitro* selection. Furthermore, the RAL-selected KP-1 variant had a completely different Env sequence from that in the passage control (particularly evident in the gp120, V1/V2 and V4-loop regions), and a different number of potential *N*-glycosylation sites. A similar pattern was also observed in other primary isolates when using different classes of drugs. This is the first study to explore the influence of anti-HIV drugs on bottlenecks in bulk primary HIV isolates with highly diverse Env sequences using *in vitro* selection.

Received 15 August 2012
Accepted 20 December 2012

INTRODUCTION

Human immunodeficiency virus type 1 (HIV-1) shows a high degree of genetic diversity owing to its high rates of replication and recombination and the high mutation rate of the HIV-1 reverse transcriptase (Nájera *et al.*, 2002). Even in a single infected individual, the virus can best be described as a population of distinct, but closely related, genetic variants or 'quasi-species' (Eigen, 1993; Nijhuis *et al.*, 1998). The quasi-species behaviour of viruses is recognized as a key element in our understanding and modelling of viral evolution and disease control (Vignuzzi *et al.*, 2006).

Combination antiretroviral (ARV) therapy results in a contraction of the viral population, which represents a potential genetic bottleneck (Charpentier *et al.*, 2006; Delwart *et al.*, 1998; Ibáñez *et al.*, 2000; Kitrinos *et al.*, 2005; Nijhuis *et al.*, 1998; Nora *et al.*, 2007; Sheehy *et al.*, 1996; Zhang *et al.*, 1994). Whilst this bottleneck has a direct effect on the region that is being targeted by the drugs (e.g. protease or reverse transcriptase), it also affects other regions of the viral genome. Indeed, the effect of the drug-induced genetic bottleneck on the population dynamics of the envelope (Env) regions has been addressed in several *in vivo* studies (Charpentier *et al.*, 2006; Delwart *et al.*, 1998; Ibáñez *et al.*, 2000; Kitrinos *et al.*, 2005; Nijhuis *et al.*, 1998; Nora *et al.*, 2007; Sheehy *et al.*, 1996; Zhang *et al.*, 1994).

Virus bottleneck evolution of the HIV-1 *env* gene might be important when choosing the optimal drugs to treat a particular patient. Indeed, a CCR5 antagonist (maraviroc, MVC) and a fusion inhibitor (enfuvirtide, T-20) have now been approved for use as HIV-1 entry inhibitors. Analysing the dynamics of drug-induced genetic bottlenecks and studying drug-resistant mutation profiles in response to

The GenBank/EMBL/DDBJ accession numbers for the *env* sequences of HIV-1 KP-1, KP-2 and KP-4, are AB640872–AB640881, AB641341–AB641351 and AB641335–AB641340, respectively.

Two supplementary figures are available with the online version of this paper.

HIV-1-specific ARV drugs are both important if we are to understand fully HIV-1 drug resistance and pathogenesis.

The aim of the present study was to understand better the effect of *in vivo* drug-induced genetic bottlenecks. *In vitro* selection of different primary HIV-1 isolates was performed using the recently approved HIV integrase inhibitor raltegravir (RAL) (Steigbigel *et al.*, 2008). Two R5-, one X4-, one dual- and one mixed R5/X4-tropic isolates were passaged through a RAL-induced genetic bottleneck. We also performed *in vitro* selection of the R5/X4 isolate using lamivudine (3TC), saquinavir (SQV) and MVC, and compared the results with those from the RAL-selected isolate.

RESULTS

Genotypic profiles of the HIV-1 primary isolates

Four genetically heterogeneous HIV-1 primary isolates (KP-1–4) from Japanese drug-naïve patients were used to assess the extent to which RAL affected the selection of bulk primary viruses *in vitro*. A laboratory isolate, strain 89.6, was also used in the study (rather than a molecular clone) to allow escape mutants to be selected from each quasi-species pool and to be generated *de novo*. First, the sequences of the integrase (IN) regions of the four primary isolates were determined. Table 1 shows the detailed evaluation of the R5/X4 mixture subtype B (KP-1), R5-CRF08_BC (KP-2), R5 subtype B (KP-3) and X4-CRF01_AE (KP-4) primary isolates, and the dual-tropic subtype B laboratory virus (89.6). Although some naturally occurring polymorphisms were observed within the IN regions of these isolates compared with the subtype B consensus sequence available from the Los Alamos National Laboratory HIV sequence database, we did not identify any primary resistant mutations to RAL. Three baseline viruses (KP-1, KP-4 and 89.6) were sensitive to RAL, with IC_{50} values ranging from 1.2 to 4 nM, which are comparable with those reported previously (Kobayashi *et al.*, 2008). However, KP-2 and KP-3 showed minor resistance to RAL, with IC_{50} values of 16 and 32 nM, respectively. These two isolates contained amino acid mutations at positions 72, 125 and 201 within the IN region [previously reported as L-870,810 and S-1360 resistance mutations (Hombrouck *et al.*, 2008; Rhee *et al.*, 2008), but not as RAL-resistance mutations]. KP-2 also contained a unique insertion at position 288 (NQDME) at the C-terminal end of the IN region.

In vitro selection of variants of the primary isolates and 89.6 using RAL

To induce RAL-selected HIV-1 variants *in vitro*, PM1/CCR5 cells, a T-cell line expressing high levels of CCR5, were exposed to the four primary isolates and strain 89.6. The viruses were then serially passaged in the presence of RAL. As a control, each isolate was passaged under the same conditions, but without RAL, to allow monitoring of spontaneous changes occurring in the viruses during prolonged PM1/CCR5 cell passage (the passage control). The selected viruses were initially propagated at a RAL concentration equal to each IC_{50} value. The RAL concentrations were then increased from 20 to 85 nM during the course of the selection procedure (Table 1).

Only small shifts in the IC_{50} to RAL were observed in four of the five isolates (KP-1, KP-2, KP-4 and 89.6), with fold changes in IC_{50} values of 3.4, 6.5, 16 and 9.2, respectively. KP-3 did not show resistance to RAL. IC_{50} values in all the passage controls were comparable with those of the baseline viruses (Table 1).

IN region sequences in RAL-selected variants

The full-length *IN* genes were amplified and cloned to determine the genetic basis of selection in the presence or absence of RAL. Ten to 12 clones from each sample were sequenced.

Substitutions within IN were observed at passages 30 (G189R) and 29 (T210I) in two RAL-selected isolates (KP-2 and KP-4, respectively). Neither of these has been reported as IN inhibitor-resistant mutations. No substitutions in the IN regions of KP-3 and 89.6 were found. However, A125T and V180I substitutions were observed in the KP-3 and 89.6 control variants at the last passage. No previously reported mutations were identified in the IN region of KP-1 (an R5/X4 mixture isolate) after 17 passages. However, four amino acids (K7/K111/H216/D278) were selected by RAL from the baseline quasi-species, whereas different amino acids (R7/R111/Q216/N278) were selected in the control-passage variants (Table 1).

Taken together, these findings showed that RAL-induced selection pressure causes adaptation within the IN regions of bulk primary viruses during *in vitro* passage in the target cells, and confirmed that this system can be used to analyse drug-selected variants *in vitro*.

Comparison of *env* gene sequences in RAL-selected and passage-control isolates

A highly diverse gp120 region was observed in the baseline R5/X4 mixture isolate, KP-1; however, the viral diversity of variants passaged in the presence or absence of RAL decreased significantly during *in vitro* selection (overall mean distance after RAL selection of 0.056 at baseline to 0.007 after passage 17; mean overall distance in the passage control of 0.01 after 20 passages, Table 2). Moreover, the RAL-selected and control variants utilized CCR5 to enter the target cell; neither variant used CXCR4 (Table 3).

Interestingly, the low-diversity RAL-selected variant contained a completely different Env sequence from that of the passage-control variant (data not shown). Different regions spanning the whole envelope sequence [from the signal peptide (SP) to V5] were compared in the RAL-selected

Table 1. Susceptibility of HIV-1 isolates to RAL and distinct differences in IN region sequences between RAL-selected and control-passaged viruses

Isolate	Subtype	Tropism	IPassage no.	RAL-selected variant*			Passage control	
				Concn (nM)	IN sequence	RAL IC_{50} (nM)	IN sequence	RAL IC_{50} (nM)
KP-1	B	Mix	0	0	*K/R7, K/R111, Q/H216, D/N278*†	4	*K/R7, K/R111, Q/H216, D/N278*	4
			8	20	**K**111, **H**216, **D**278‡	31	**R**7, **R**111, **Q**216, **N**278	4.5 (1.2)
			17†	20	**K**7, **K**111, **H**216, **D**278	26 (6.5)	**R**7, **R**111, **Q**216, **N**278	0.4 (0.1)
KP-2	CRF08_BC	R5	0	0	*I201, ins289NQDME*	16	*I201, ins289NQDME*	16 (1)
			18	40	G189G/R, *I201, ins289NQDME*	32 (2)	*I201, ins289NQDME*	16
			30	85	G189R, *I201, ins289NQDME*	55 (3.4)	*I201, ins289NQDME*	25 (1.6)
KP-3	B	R5	0	0	*V72, A125*	32	*V72, A125*	32
			11	25	*V72, A125*	25	*V72, A125*	33 (1)
			22	27.5	*V72, A125*	37 (1.2)	*V72,* A125T	13
KP-4	CRF01_AE	X4	0	0	–	2.1	–	2.1
			8	40	–	33 (16)	R166R/K, D279N	4.4 (2.1)
			29	40	T210I	22 (10)	G163E, R166R/K, D279N/S	4.1 (2)
89.6	B	R5X4	0	0	–	1.2	–	1.2
			8	15	–	34 (28)	–	4.4 (3.7)
			34	20	–	11 (9.2)	V180I	1.2 (1)

*Amino acid changes in each passage variant are shown. Italicized letters represent mutations relative to the consensus subtype BC or B present in the baseline isolates. Bold letters represent amino acids selected out of the quasi-species cloud. The fold increase in RAL IC_{50} values is shown for *in vitro*-selected variants compared with those in the baseline isolates.
†The RAL variant selected after 17 passages was compared with the control selected after 20 passages.

Table 2. Comparison of amino acid length and number of PNGs between RAL-selected and control-passage KP-1 variants

	Passage no.	Genetic diversity*	Mean ENV $_{1-474}$ length (range)†	Mean V1/V2 length (range)	Mean V3 length (range)	Mean V4 length (range)	Mean PNGs (range)
Base line	0	0.056	472 (461–480)	69 (60–74)	34 (33–34)	30 (29–31)	24 (22–28)
RAL-selected virus	2	0.038	479 (472–480)‡	74 (71–74)‡	34 (33–34)‡	31 (29–31)‡	27 (25–28) ‡
	8	0.0070	480	74	34	31	28 (26–29)
	17	0.0070	480	74	34	31	27 (26–27)§
Passage control	2	0.045	464 (461–466)‡	64 (60–74)‡	34 (33–34)‡	29 (29–31)‡	24 (22–27)‡
	8	0.0070	463 (462–463)	62	34	29	23 (22–23)
	10	0.0080	462 (459–463)	62	34	29	23 (22–23)
	20	0.010	463	62	34	29	23 (22–23)§
P value			<0.0001‡	<0.0001‡	0.91‡	0.0048‡	0.0019‡ <0.0001§

*Overall mean distance.
†Sequence from gp120 SP to the V5 region (aa 1–474).
‡, § *P* values were calculated using the homoscedastic *t*-test between the RAL-selected and the passage-control variants indicated by the same symbols above.

and passage-control viruses. The results showed that, after only two passages, the gp120, V1/V2 and V4-loop regions within RAL-selected variants were longer than those in the control variants, and the number of putative *N*-linked glycosylation sites (PNGs) was significantly higher than that in the control-passage viruses (Table 2). This phenomenon was seen consistently in two independent experiments.

We also analysed the gp120 sequences in the other four isolates. Although the number of positional differences between the RAL-selected and passage-control variants for these four isolates was lower than that in KP-1 (between three and nine, compared with >40), there was a similar pattern of separation between the Env sequences (Fig. 1). In three of the four isolates (KP-2, KP-3 and KP-4), positional differences were observed in SP, C1 and all the variable regions of gp120 (Fig. 1b–d). In strain 89.6, differences were observed in the C2, C3 and V4 regions (Fig. 1e).

These results suggested that RAL treatment of target cells causes a decrease in viral diversification within quasi-species Env regions via a route different from that in untreated target cells.

In vitro induction of RAL-selected V3-loop library virus variants

To investigate further the effects of RAL on viral Env sequences, we used the V3-loop library virus (JR-FL-V3Lib) developed by Yusa *et al.* (2005), which carries a set of random combinations from zero to ten substitutions (27 648 possibilities) in the V3 loop (residues 305, 306, 307, 308, 309, 317, 319, 322, 323 and 326; V3 loop from Cys^{296} to Cys^{331}). The variants contained in the library were polymorphic mutations derived from 31 R5 clinical isolates (Yusa *et al.*, 2005). PM1/CCR5 cells were exposed to the JR-FL-V3Lib and serially passaged in the presence of RAL. After two passages, the V3 sequence within the RAL-selected variant was completely different from that in the passage control (Fig. 1f). This suggested that, under pressure from RAL, the infectious clone harbouring different V3 region sequence from the passage control had adapted to the target cells, despite containing the same IN sequences.

Phylogenetic analysis of the Env regions after passage with or without RAL

To confirm the temporal and spatial differences observed in each of the RAL-selected and passage-control viruses, phylogenetic analyses were conducted using complete SP–V5 sequences. The neighbour-joining phylogenetic tree showed a clear and distinct branching between RAL-selected and passage-control KP-1 viruses (Fig. 2a). We also identified a similar pattern in all the other isolates tested (Fig. 2b–e).

Table 3. Comparison of amino acid length, number of potential *N*-linked glycosylation sites, V3 sequences and co-receptor usage between anti-retroviral drug-selected and control-passaged KP-1 variants

	Passage no.	Genetic diversity*	Mean ENV_{1-474} length (range)†	Mean V1/V2 length (range)	Mean V3 length (range)	Mean V4 length (range)	Mean PNGs (range)	V3 region		Geno2 pheno (%)§
								Prevalence (%)	Sequence‡	
Base line	0	0.056	472 (461–480)	69 (60–74)	34 (33–34)	30 (29–31)	24 (22–28)	41.9	CTRPNNNTRKGIHIGPGKFYATGAIIGDIRQAHC	41.2
								22.6	.....V.....	41.2
								16.1	....-..I.....T.R..T.RD...N..K...	1.7
								13.0	....-..I.....T.R..T.KT...N.KK...	2.9
								3.2	....-..I.....	7.4
								3.2	.....D.....	55.3
Passage control	8	0.0070	463 (462–463)	62	34	29	23 (22–23)	100.0	.....V.....	41.2
RAL-selected virus	8	0.0070	480	74	34	31	28 (26–29)	100.0	.....	41.2
3TC-selected virus	6	0.020	478 (475–480)	74	34	31 (29–31)	27 (25–28)	83.3	.....	41.2
SQV-selected virus	11	0.0040	474	71	34	31	26	100.0	.....	41.2
MVC-selected virus	7	0.0080	469 (468–469)	69	33	29	24 (23–24)	100.0	....-..I....R..T.R..T.KT...N.KK...	1.7

*Overall mean distance.

†Sequence from gp120 SP to the V5 region (aa 1–474).

‡V3 sequences of each variant are shown. Dots denote sequence identity and dashes indicate a deletion mutation.

§Prediction of viral co-receptor tropism using Geno2pheno based on a selectable 'false positive rate'.

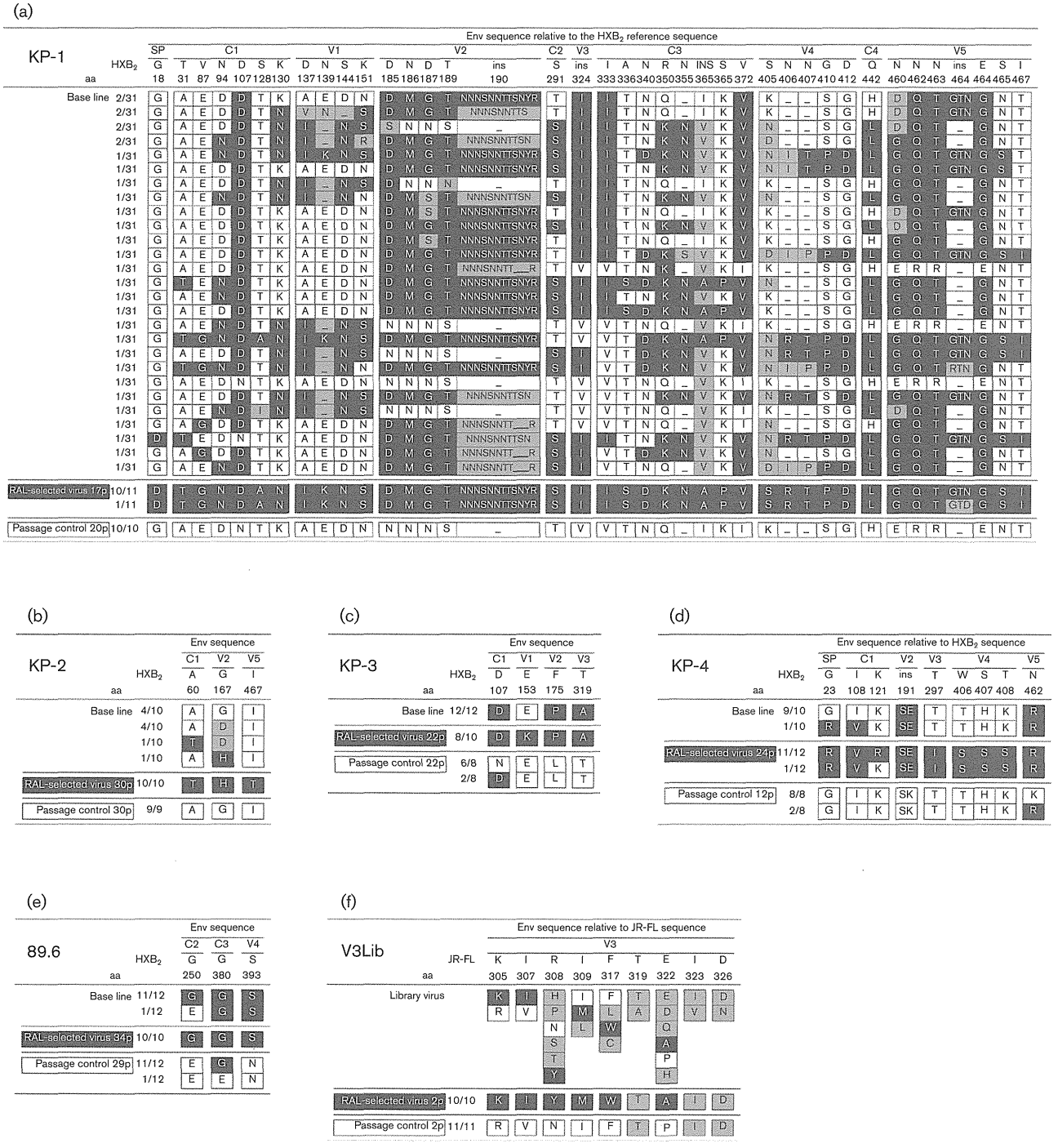

Fig. 1. Comparison of the gp120 sequences between RAL-selected and control-passaged viruses. The gp120 sequences of baseline, RAL-selected and the passage-control viruses were aligned for KP-1 (a), KP-2 (b), KP-3 (c), KP-4 (d) and strain 89.6 (e). Each amino acid in (a)–(e) is numbered relative to the HIV-1 HXB_2 reference sequence. The V3 sequences from the JR-FL-V3Lib baseline library, RAL-selected and passage-control viruses were aligned (f). Filled cells denote the most dominant amino acids observed in RAL-selected variants at the latest passage, open cells denote the most dominant amino acids observed in the passage-control variants at the latest passage and shaded cells show amino acids deleted by the end of both passages, whilst '–' indicates a deletion mutation. The number of passages is indicated, e.g. 17p for passage 17.

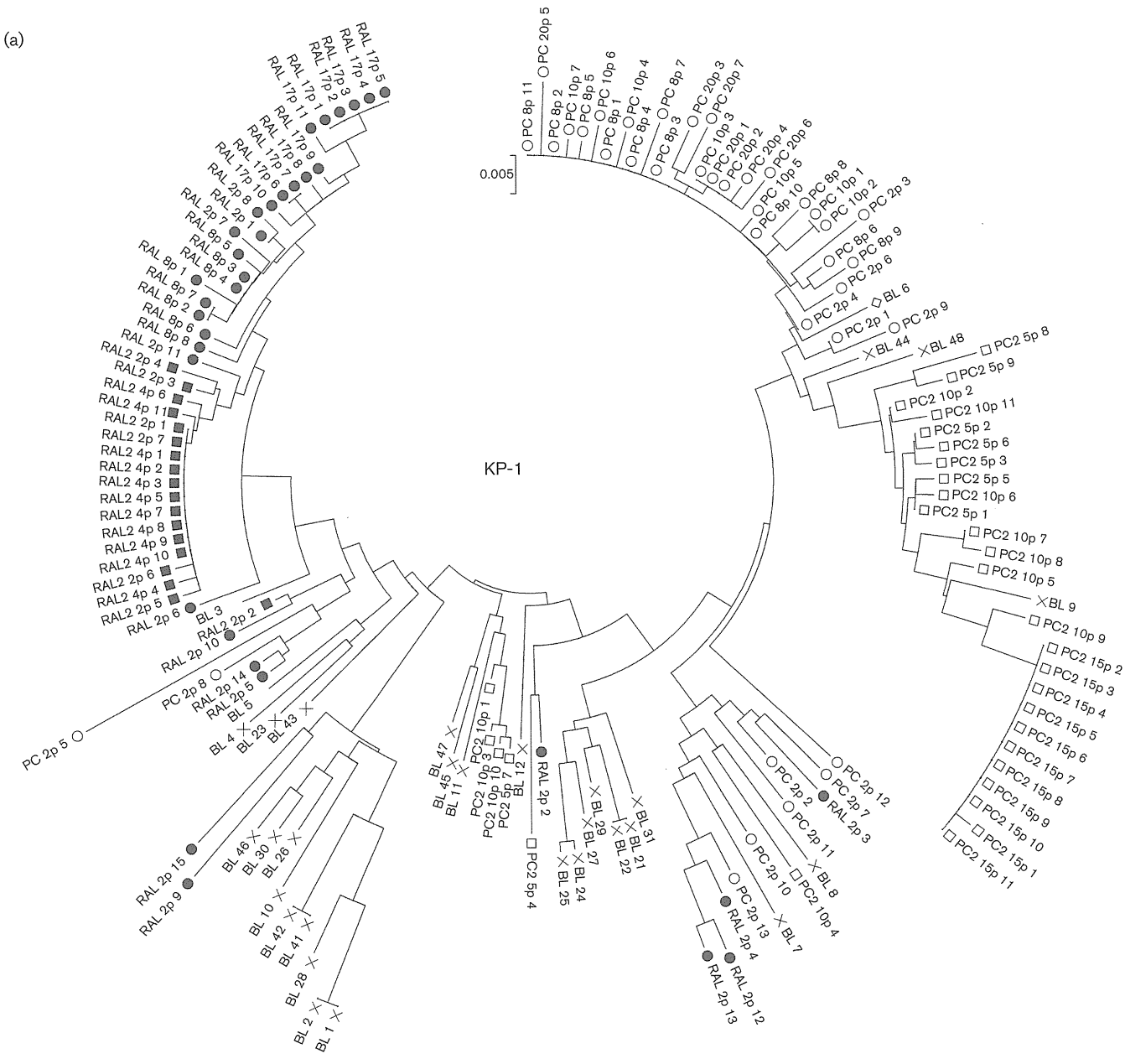

Fig. 2. Phylogenetic analyses of the Env regions from *in vitro*-passaged viruses selected with or without ARV drugs. (a–e) Phylogenetic trees were constructed using gp120 SP–V5 sequences from RAL-selected and passage-control variants of KP-1 (a), KP-2 (b), KP-3 (c), KP-4 (d) and strain 89.6 (e). An '×' represents baseline (BL) variants, and closed and open symbols represent RAL-selected (RAL) and passage-control (PC) variants, respectively. In (a), the results of the second experiment are indicated RAL2 and PC2, respectively. (f) A phylogenetic tree was constructed using gp120 SP–V5 sequences from RAL-, 3TC-, SQV-, MVC-selected and control-passaged variants of KP-1 (f). ○, Control variants after eight passages; ●, RAL-selected variants after eight passages; ▲, 3TC-selected variants after six passages; ◆, SQV-selected variants after 11 passages; ■, MVC-selected variants after seven passages. The trees were constructed using the neighbour-joining algorithm embedded within the MEGA software.

In vitro selection of KP-1 variants by 3TC, SQV and MVC

To determine whether other HIV drugs also changed the route of adaptation to the target cells, we attempted to select KP-1 variants using a reverse transcriptase inhibitor (3TC), a protease inhibitor (SQV) and a CCR5 inhibitor (MVC). As shown in Fig. 2(f), the pattern of clustering at distinct positions between the selected isolates and the passage-control variants was similar to that observed for

the RAL-selected variants. The selected variants showed decreased diversity in the gp120 sequences; however, the length of the gp120, V1/V2 and V4 sequences increased (apart from in the MVC-selected variants). In addition, the number of PNGs within gp120 was higher than that in the control (Table 3). We also compared the V3 sequences between the passage-control and each of the drug-selected variants. The V3 sequences in all the SQV-selected variants and 83.3 % of those in the 3TC-selected variants, were comparable with those in the RAL-selected variants. This was not the case for the passage controls. Comparison of variants passaged with RAL and 3TC showed that the length of the V1/V2 and V4 regions and the number of PNGs was similar; however, these parameters were different in the SQV-selected variants (Table 3). This indicated that the time at which a drug acts (e.g. during the early or late phase of the HIV life cycle) influences the selection of Env sequences. During selection with MVC, CXCR4-tropic variants were selected from the baseline mixture after seven passages.

Taken together, these results suggested that, in treated cells, different classes of anti-HIV drugs may suppress the variability of quasi-species during *in vitro* selection via a route different from that in untreated cells.

DISCUSSION

This study evaluated the impact of anti-HIV drugs on the Env bottleneck in bulk HIV-1 primary isolates during selection *in vitro*. RAL-, 3TC- and SQV-selected variants of the unique viral isolate, KP-1, harbouring both X4 and R5 variants and with a very high level of baseline viral diversity, were used to study the final destination (genetic bottleneck) of a large variety of Env sequences. Interestingly, the phylogenetic clustering of RAL-selected KP-1 variants was completely different from that of non-drug-treated controls (Fig. 2). Our results also confirmed differences in the length of the gp120, V1/V2 and V4-loop regions and in the number of PNGs (Tables 2 and 3).

It is not clear why viruses cultured under pressure from the non-Env-directed drug RAL result in different *env* genotypes compared with those without the drug. Thus, we cloned the *IN–env* region of the proviral genome from passaged viruses and sequenced the *env* and *IN* regions on the same cloned plasmid, and compared them among the baseline and passages 1, 2, 8 and 17 of the KP-1 virus. Under low concentrations of the IN inhibitor RAL, K7 was selected for at a late passage after accumulation of the other three amino acids, K111, D278 and H216, in IN. During the sequential accumulation of these four amino acids (K111, D278, H216 and K7), the RAL-selected Env sequences at passage 17 (the Env sequences shown as filled boxes shown in Fig. 1) sequentially accumulated mutations in the same proviral genome. However, we did not find a clone including both the RAL-selected Env at passage 17 and RAL-selected IN at passage 17 in the baseline or each passaged virus, except for in the last passage. We also examined the gp120 and IN sequences of the 3TC- and SQV-selected KP-1 variants. Compared with the RAL-selected region, the variable regions of gp120 in these selected variants were very similar to each other, except for the V1/V2 region (Fig. S2). However, the passage-control variant was very different from the drug-selected variants (Fig. 1a). Furthermore, the IN sequences were different in each passaged virus: K111/D278/H216/K7 in RAL-selected, R111/D278/Q216/R7 in 3TC-selected, K111/D278/H216/R7 in SQV-selected and R111/N278/Q216/R7 in virus without drug treatment (underlined residues indicate amino acids different from those in viruses without drug treatment). To explain these results, we believe that, under pressure from anti-HIV drugs (non-entry ARVs), the virus might show a primitive reaction to select for the Env sequence and recombine from quasi-species to gain advantage for entry and/or enhance replication in target cells. Meanwhile, IN was selected from quasi-species by a direct and/or indirect effect of RAL-induced pressure. The combination of both selective pressures may affect the selection for Env and IN during adaptation in drug-treated conditions (Figs 1a and S2). These results suggest that non-entry inhibitors, such as RAL, 3TC and SQV, might also affect cell adaptation to PM1/CCR5 cells.

Many *in vivo* studies have reported the effects of the anti-HIV drug-induced bottleneck on the *env* gene (Charpentier *et al.*, 2006; Delwart *et al.*, 1998; Ibáñez *et al.*, 2000; Kitrinos *et al.*, 2005; Nijhuis *et al.*, 1998; Nora *et al.*, 2007; Sheehy *et al.*, 1996; Zhang *et al.*, 1994). However, these studies had several limitations. Because viruses were placed under *in vivo* selective pressure using at least two anti-HIV drugs and by the host immune response, it is difficult to separate the different effects and to draw clear conclusions, particularly *in vivo*. Delwart *et al.* (1998) and Kitrinos *et al.* (2005) avoided some of these limitations by employing a heteroduplex tracking assay, although *in vivo* peculiarities still remained. Therefore, we used an *in vitro* selection system using unique bulk primary isolates established in our laboratory (Hatada *et al.*, 2010; Shibata *et al.*, 2007; Yoshimura *et al.*, 2006, 2010b) to observe the effects of the anti-retroviral drug-induced bottleneck on the *IN* and *env* genes.

This selection provides a sensitive approach for analysing virus population dynamics. The effectiveness of ARV drugs can be examined during the *in vitro* passage of a single variant or mixture of variants without being affected by many of the factors encountered *in vivo*. In addition, differences in the Env sequences between the baseline and selected variants can be compared after any number of passages. The results of the present study provide important information that will enhance our understanding of the drug-induced genetic bottleneck. This phenomenon can be examined *in vitro* using bulk primary isolates treated with or without drugs.

Recently, several new ARV drugs have been licensed for use in HIV-1-infected patients. MVC, approved in 2006, is the

first CCR5 inhibitor (Gulick *et al.*, 2008). One important advantage associated with this drug is the absence of cross-resistance with previously available ARV compounds (Gulick *et al.*, 2008; Steigbigel *et al.*, 2008). However, as is usual with anti-HIV drugs, resistant variants with mutations in the Env, gp120 and gp41 sequences are induced both *in vivo* and *in vitro* (Anastassopoulou *et al.*, 2009; Berro *et al.*, 2009; Tilton *et al.*, 2010; Yoshimura *et al.*, 2009, 2010a). As shown in the present study, distinct Env sequences from each quasi-species might be selected by the different anti-HIV drugs (e.g. length of the V1/2 and/or V4 regions, V3 region depletion and the number of PNGs). Moreover, many of the novel anti-retroviral drugs in pre-clinical trials are viral entry inhibitors (e.g. PRO140, ibalizumab, BMS-663068 and PF-232798; Jacobson *et al.*, 2010; McNicholas *et al.*, 2010; Nettles *et al.*, 2011; Stupple *et al.*, 2011; Toma *et al.*, 2011). Therefore, it is necessary to examine whether such entry inhibitors are effective when used alongside conventional drugs.

In conclusion, we studied the genetic bottleneck in bulk primary HIV-1 isolates from untreated patients and drugs targeting the Env (and other) regions. The results showed, for the first time, the presence of drug-selected Env sequences in these isolates. Although our observations were based on a limited number of HIV-1 isolates and need to be confirmed by independent studies, we believe that they provide a new paradigm for HIV-1 evolution in the new combination ARV therapy era.

METHODS

Patients and isolates. Primary HIV-1 isolates were isolated from four drug-naïve patients in our laboratory (KP-1–4) and passaged in phytohaemagglutinin-activated PBMCs. Infected PBMCs were then co-cultured for 5 days with PM1/CCR5 cells (a kind gift from Dr Y. Maeda; Maeda *et al.*, 2008; Yusa *et al.*, 2005) and the culture supernatants were stored at −150 °C (Hatada *et al.*, 2010; Shibata *et al.*, 2007; Yoshimura *et al.*, 2006, 2010b).

After isolation of the primary viruses, we checked the sensitivity of each primary isolate to MVC. The KP-1 isolate was relatively MVC-resistant compared with KP-2 and KP-3 (54 vs 5.9 and 8.7 nM, respectively). KP-1 became MVC sensitive after eight passages in PM1/CCR5 cells [IC_{50}, 3.4 nM; Geno2pheno value (see below), 41.2 %], whilst under the pressure of MVC, KP-1 became highly resistant to MVC after eight passages (IC_{50}, >1000 nM; Geno2pheno value, 1.7 %). These results indicated that the bulk KP-1 isolate used in this study harboured primarily R5 viruses with X4- or dual-tropic viruses as a minor population.

Cells, culture conditions and reagents. PM1/CCR5 cells were maintained in RPMI 1640 (Sigma) supplemented with 10 % heat-inactivated FCS (HyClone Laboratories), 50 U penicillin ml^{-1}, 50 μg streptomycin ml^{-1} and 0.1 mg G418 (Nacalai Tesque) ml^{-1}. MVC, RAL and SQV were kindly provided by Pfizer, Merck & Co. and Roche Products, respectively. 3TC was purchased from Wako Pure Chemical Industries.

The laboratory-adapted HIV-1 strain 89.6, which was obtained through the NIH AIDS Research and Reference Reagent Program, was propagated in phytohaemagglutinin-activated PBMCs. The viral-competent library pJR-FL-V3Lib, which contains 176 bp V3–loop DNA fragments with 0–10 random combinations of amino acid substitutions, was introduced into pJR-FL, as described previously (Yusa *et al.*, 2005).

***In vitro* selection of HIV-1 variants using anti-HIV drugs.** The four primary HIV isolates (KP-1–4), strain 89.6 and JR-FL-V3Lib were treated with various concentrations of RAL and used to infect PM1/CCR5 cells to induce the production of RAL-selected HIV-1 variants, as described previously, with minor modifications (Hatada *et al.*, 2010; Shibata *et al.*, 2007; Yoshimura *et al.*, 2006, 2010b). Briefly, PM1/CCR5 cells (4×10^4 cells) were exposed to 500 $TCID_{50}$ HIV-1 isolates and cultured in the presence of RAL. Virus replication in PM1/CCR5 cells was monitored by observing the cytopathic effects. The culture supernatant was harvested on day 7 and used to infect fresh PM1/CCR5 cells for the next round of culture in the presence of increasing concentrations of RAL. When the virus began to propagate in the presence of the drug, the compound concentration was increased further. Proviral DNA was extracted from lysates of infected cells at different passages using a QIAamp DNA Blood Mini kit (Qiagen). The proviral DNAs obtained were then subjected to nucleotide sequencing. *In vitro* selection of the KP-1 isolate using SQV, 3TC and MVC was also performed using the procedure described above.

Amplification of proviral DNA and nucleotide sequencing. Proviral DNA was subjected to PCR amplification using PrimeSTAR GXL DNA polymerase and Ex-*Taq* polymerase (Takara), as described previously (Hatada *et al.*, 2010; Shibata *et al.*, 2007; Yoshimura *et al.*, 2006, 2010b). The primers used were 1B and H for the gp120 region (Hatada *et al.*, 2010; Shibata *et al.*, 2007; Yoshimura *et al.*, 2006, 2010b), IN 1F (5′-CAGACTCACAATATGCATTAGG-3′) and IN 1R (5′-CCTGTATGCAGACCCCAATATG-3′) for the *IN* region, and IN 1F and H for the *IN*–gp120 region. The first-round PCR products were used directly in a second round of PCR using primers 2B and F (Hatada *et al.*, 2010; Shibata *et al.*, 2007; Yoshimura *et al.*, 2006, 2010b) for gp120, IN 2F (5′-CTGGCATGGGTACCAGCACACAA-3′) and IN 2R (3′-CCTAGTGGGATGTGTACTTCTGAACTTA-3′) for *IN*, and IN 2F and F for *IN*–gp120. The PCR conditions used were as described above. The second-round PCR products were purified and cloned into a pGEM-T Easy Vector (Promega) or pCR-XL-TOPO Vector (Invitrogen), and the *env* and *IN* regions in both the passaged and selected viruses were sequenced using an Applied Biosystems 3500xL Genetic Analyzer and a BigDye Terminator v3.1 Cycle Sequencing kit (Applied Biosystems). Phylogenetic reconstructions were generated using the neighbour-joining method embedded in the MEGA software (http://www.megasoftware.net) (Tamura *et al.*, 2007). Overall, mean distances for viral diversity were also calculated using MEGA software. The number and location of putative PNGs were estimated using *N*-GlycoSite (http://www.hiv.lanl.gov/content/sequence/GLYCOSITE/glycosite.html) from the Los Alamos National Laboratory database.

Susceptibility assay. The sensitivity of the passaged viruses to various drugs was determined as described previously with minor modifications (Hatada *et al.*, 2010; Shibata *et al.*, 2007; Yoshimura *et al.*, 2006, 2010b). Briefly, PM1/CCR5 cells (2×10^3 cells per well) in 96-well round-bottomed plates were exposed to 100 $TCID_{50}$ of the viruses in the presence of various concentrations of drugs and incubated at 37 °C for 7 days. The IC_{50} values were then determined using a Cell Counting Kit-8 assay (Dojindo Laboratories). All assays were performed in duplicate or triplicate.

Predicting co-receptor usage by the V3 sequence. HIV-1 tropism was inferred using Geno2pheno [coreceptor] program, with a false rate positive (FPR) value of 5.0 %, which is freely available (http://coreceptor.bioinf.mpi-inf.mpg.de/index.php). This genotyping tool more accurately predicts virological responses to the CCR5

antagonist MVC in ARV-naïve patients than a reference phenotypic tropism test (Sing *et al.*, 2007).

Statistical analyses. Pairwise comparisons of the different parameters between variants in the two groups was calculated using the homoscedastic *t*-test. A P value of <0.05 was considered statistically significant.

ACKNOWLEDGEMENTS

We are grateful to Dr Yosuke Maeda for providing the PM1/CCR5 cells. We also thank Syoko Yamashita, Yoko Kawanami, Noriko Shirai, and Akiko Shibata for technical assistance. This study was supported in part by the Ministry of Education, Culture, Sports, Science and Technology, Japan, by a Grant-in-Aid for Young Scientists (B-22790163); grants from the Ministry of Health, Labour and Welfare; the Program of Founding Research Centers for Emerging and Re-emerging Infectious Diseases; and the Global COE program Global Education and Research Center Aiming at the Control of AIDS.

REFERENCES

Anastassopoulou, C. G., Ketas, T. J., Klasse, P. J. & Moore, J. P. (2009). Resistance to CCR5 inhibitors caused by sequence changes in the fusion peptide of HIV-1 gp41. *Proc Natl Acad Sci U S A* **106**, 5318–5323.

Berro, R., Sanders, R. W., Lu, M., Klasse, P. J. & Moore, J. P. (2009). Two HIV-1 variants resistant to small molecule CCR5 inhibitors differ in how they use CCR5 for entry. *PLoS Pathog* **5**, e1000548.

Charpentier, C., Nora, T., Tenaillon, O., Clavel, F. & Hance, A. J. (2006). Extensive recombination among human immunodeficiency virus type 1 quasispecies makes an important contribution to viral diversity in individual patients. *J Virol* **80**, 2472–2482.

Delwart, E. L., Pan, H., Neumann, A. & Markowitz, M. (1998). Rapid, transient changes at the *env* locus of plasma human immunodeficiency virus type 1 populations during the emergence of protease inhibitor resistance. *J Virol* **72**, 2416–2421.

Eigen, M. (1993). The origin of genetic information: viruses as models. *Gene* **135**, 37–47.

Gulick, R. M., Lalezari, J., Goodrich, J., Clumeck, N., DeJesus, E., Horban, A., Nadler, J., Clotet, B., Karlsson, A. & other authors (2008). Maraviroc for previously treated patients with R5 HIV-1 infection. *N Engl J Med* **359**, 1429–1441.

Hatada, M., Yoshimura, K., Harada, S., Kawanami, Y., Shibata, J. & Matsushita, S. (2010). Human immunodeficiency virus type 1 evasion of a neutralizing anti-V3 antibody involves acquisition of a potential glycosylation site in V2. *J Gen Virol* **91**, 1335–1345.

Hombrouck, A., Voet, A., Van Remoortel, B., Desadeleer, C., De Maeyer, M., Debyser, Z. & Witvrouw, M. (2008). Mutations in human immunodeficiency virus type 1 integrase confer resistance to the naphthyridine L-870,810 and cross-resistance to the clinical trial drug GS-9137. *Antimicrob Agents Chemother* **52**, 2069–2078.

Ibáñez, A., Clotet, B. & Martinez, M. A. (2000). Human immunodeficiency virus type 1 population bottleneck during indinavir therapy causes a genetic drift in the env quasispecies. *J Gen Virol* **81**, 85–95.

Jacobson, J. M., Thompson, M. A., Lalezari, J. P., Saag, M. S., Zingman, B. S., D'Ambrosio, P., Stambler, N., Rotshteyn, Y., Marozsan, A. J. & other authors (2010). Anti-HIV-1 activity of weekly or biweekly treatment with subcutaneous PRO 140, a CCR5 monoclonal antibody. *J Infect Dis* **201**, 1481–1487.

Kitrinos, K. M., Nelson, J. A., Resch, W. & Swanstrom, R. (2005). Effect of a protease inhibitor-induced genetic bottleneck on human immunodeficiency virus type 1 *env* gene populations. *J Virol* **79**, 10627–10637.

Kobayashi, M., Nakahara, K., Seki, T., Miki, S., Kawauchi, S., Suyama, A., Wakasa-Morimoto, C., Kodama, M., Endoh, T. & Oosugi, E. (2008). Selection of diverse and clinically relevant integrase inhibitor-resistant human immunodeficiency virus type 1 mutants. *Antiviral Res* **80**, 213–222.

Maeda, Y., Yusa, K. & Harada, S. (2008). Altered sensitivity of an R5X4 HIV-1 strain 89.6 to coreceptor inhibitors by a single amino acid substitution in the V3 region of gp120. *Antiviral Res* **77**, 128–135.

McNicholas, P., Wei, Y., Whitcomb, J., Greaves, W., Black, T. A., Tremblay, C. L. & Strizki, J. M. (2010). Characterization of emergent HIV resistance in treatment-naive subjects enrolled in a vicriviroc phase 2 trial. *J Infect Dis* **201**, 1470–1480.

Nájera, R., Delgado, E., Pérez-Alvarez, L. & Thomson, M. M. (2002). Genetic recombination and its role in the development of the HIV-1 pandemic. *AIDS* **16** (Suppl. 4), S3–S16.

Nettles, R., Schurmann, D., Zhu, L., Stonier, M., Huang, S. P., Chien, C., Krystal, M., Wind-Rotolo, M., Bertz, R. & Grasela, D. (2011). Pharmacodynamics, safety, and pharmacokinetics of BMS-663068: a potentially first-in-class oral HIV attachment inhibitor. In *18th Conference on Retroviruses and Opportunistic Infections*, abstract 49. Boston, MA.

Nijhuis, M., Boucher, C. A., Schipper, P., Leitner, T., Schuurman, R. & Albert, J. (1998). Stochastic processes strongly influence HIV-1 evolution during suboptimal protease-inhibitor therapy. *Proc Natl Acad Sci U S A* **95**, 14441–14446.

Nora, T., Charpentier, C., Tenaillon, O., Hoede, C., Clavel, F. & Hance, A. J. (2007). Contribution of recombination to the evolution of human immunodeficiency viruses expressing resistance to antiretroviral treatment. *J Virol* **81**, 7620–7628.

Rhee, S.-Y., Liu, T. F., Kiuchi, M., Zioni, R., Gifford, R. J., Holmes, S. P. & Shafer, R. W. (2008). Natural variation of HIV-1 group M integrase: implications for a new class of antiretroviral inhibitors. *Retrovirology* **5**, 74.

Sheehy, N., Desselberger, U., Whitwell, H. & Ball, J. K. (1996). Concurrent evolution of regions of the envelope and polymerase genes of human immunodeficiency virus type 1 observed during zidovudine (AZT) therapy. *J Gen Virol* **77**, 1071–1081.

Shibata, J., Yoshimura, K., Honda, A., Koito, A., Murakami, T. & Matsushita, S. (2007). Impact of V2 mutations on escape from a potent neutralizing anti-V3 monoclonal antibody during in vitro selection of a primary human immunodeficiency virus type 1 isolate. *J Virol* **81**, 3757–3768.

Sing, T., Low, A. J., Beerenwinkel, N., Sander, O., Cheung, P. K., Domingues, F. S., Büch, J., Däumer, M., Kaiser, R. & other authors (2007). Predicting HIV coreceptor usage on the basis of genetic and clinical covariates. *Antivir Ther* **12**, 1097–1106.

Steigbigel, R. T., Cooper, D. A., Kumar, P. N., Eron, J. E., Schechter, M., Markowitz, M., Loutfy, M. R., Lennox, J. L., Gatell, J. M. & other authors (2008). Raltegravir with optimized background therapy for resistant HIV-1 infection. *N Engl J Med* **359**, 339–354.

Stupple, P. A., Batchelor, D. V., Corless, M., Dorr, P. K., Ellis, D., Fenwick, D. R., Galan, S. R., Jones, R. M., Mason, H. J. & other authors (2011). An imidazopiperidine series of CCR5 antagonists for the treatment of HIV: the discovery of N-(1S)-1-(3-fluorophenyl)-3-[(3-endo)-3-(5-isobutyryl-2-methyl-4,5,6,7-tetrahydro-1H-imidazo[4,5-c]pyridin-1-yl)-8-azabicyclo[3.2.1]oct-8-yl]propylacetamide (PF-232798). *J Med Chem* **54**, 67–77.